Fullerene−Oligophenylenevinylene Hybrids: Synthesis, Electronic Properties, and Incorporation in Photovoltaic Devices

Jean-François Eckert, Jean-François Nicoud, and Jean-François Nierengarten*

Contribution from the Institut de Physique et de Chimie des Matériaux de Strasbourg, Groupe des Matériaux Organiques, Université Louis Pasteur and CNRS, 23 rue du Loess, 67037 Strasbourg, France

Sheng-Gao Liu and Luis Echegoyen*

Department of Chemistry, University of Miami, Coral Gables, Florida 33124

Francesco Barigelletti and Nicola Armaroli*

Istituto di Fotochimica e Radiazioni d'Alta Energia del CNR, via Gobetti 101, 40129 Bologna, Italy

Lahoussine Ouali, Victor Krasnikov, and Georges Hadziioannou*

Department for Polymer Chemistry and Materials Science Center, University of Groningen, Nijenborgh 4, 9747 AG Groningen, The Netherlands

Received November 22, 1999. Revised Manuscript Received May 31, 2000

Abstract: Fullerene derivatives in which an oligophenylenevinylene (OPV) group is attached to C_{60} through a pyrrolidine ring have been prepared by 1,3-dipolar cycloaddition of the azomethine ylides generated in situ from the corresponding aldehydes and sarcosine. Electrochemical and photophysical studies have revealed that ground-state electronic interactions between the covalently bonded OPV moiety and the fullerene sphere are small. The photophysical investigations have also shown that both in dichloromethane and benzonitrile solution an efficient singlet−singlet OPV → C_{60} photoinduced energy-transfer process takes place, and occurrence of electron transfer, if any, is by far negligible relative to energy transfer. The C_{60}−OPV derivatives have been incorporated in photovoltaic devices, and a photocurrent could be observed showing that photoinduced electron transfer does take place under these conditions. However, the efficiency of the devices is limited by the fact that photoinduced electron transfer from the OPV moiety to the C_{60} sphere must compete with an efficient energy transfer. The latter process, as studied in solution, leads to the population of the fullerene lowest singlet excited state, found to lie slightly lower in energy than the charge-separated state expected to yield electron/hole pairs. Thus, only a small part of the absorbed light is able to contribute effectively to the photocurrent.

Introduction

Organic semiconducting materials are currently being intensively investigated in photovoltaic cells with the aim of generating large-area photodetectors[1] and solar cells.[2,3] The photovoltaic effect involves the production of electrons and holes in a semiconductor device under illumination and their subsequent collection at opposite electrodes. In organic semiconductors, photoabsorption creates bound electron−hole pairs—so-called "excitons"—so that charge collection requires their dissociation. Efficient exciton dissociation often occurs at the interface between the conjugated polymer and the metal electrode due to the different electron affinities and ionization potentials. Since the diffusion length of the excitons in these polymers is in the range of 10 nm, only a small part of the photogenerated pairs will be able to reach the polymer/metal interface and thus contribute to the photocurrent.

Recently, a novel concept for photovoltaic devices, based on interpenetrating blends of donors and acceptors sandwiched between two asymmetric contacts (two metals with different work functions), has been proposed.[2] When the donor is excited, the electron promoted to the lowest unoccupied molecular orbital (LUMO) will lower its energy by moving to the LUMO of the acceptor. Under the influence of the built-in electric field caused by the asymmetric contacts, separation of the opposite charges takes place, with the holes being transported in the donor phase and the electrons in the acceptor. In this way, the blend can be considered as a network of donor−acceptor heterojunctions that allows efficient exciton dissociation and balanced bipolar transport throughout its whole volume. The observation of

† E-mail: niereng@ipcms.u-strasbg.fr. Tel: (33) 3 88 10 71 63. Fax: (33) 3 88 10 72 46.

(1) Sariciftci, N. S.; Braun, D.; Zhang, C.; Srdanov, V.; Heeger, A. J.; Stucky, G.; Wudl, F. *Appl. Phys. Lett*. **1993**, *62*, 585. Yu, G.; Pakbaz, K.; Heeger, A. J. *Appl. Phys. Lett*. **1994**, *64*, 3422. Yu, G.; Wang, J.; McElvain, J.; Heeger, A. J. *Adv. Mater*. **1998**, *10*, 1431.

(2) Halls, J. J. M.; Walsh, C. A.; Greenham, N. C.; Marseglia, E. A.; Friend, R. H.; Moratti, S. C.; Holmes, A. B. *Nature* **1995**, *376*, 498. Yu, G.; Gao, J.; Hummelen, J. C.; Wudl, F.; Heeger, A. J. *Science* **1995**, *270*, 1789.

(3) Roman, L. S.; Andersson, M. R.; Yohannes, T. Inganäs, O. *Adv. Mater*. **1997**, *9*, 1164. Granström, M.; Petritsch, K.; Arias, A. C.; Lux, A.; Andersson, M. R.; Friend, R. H. *Nature* **1998**, *395*, 257; Roman, L. S.; Mammo, W.; Pettersson, L. A. A.; Andersson, M. R.; Inganäs, O. *Adv. Mater*. **1998**, *10*, 774.

10.1021/ja9941072 CCC: $19.00
Published on Web 07/21/2000

reversible, metastable photoinduced electron transfer from conjugated oligomers and/or polymers to C_{60}[4] has attracted fair attention in view of its potential application in photovoltaic devices.

The performance of this type of device is very sensitive to the morphology of the blend. Ideally (to ensure efficient exciton dissociation), an acceptor species should be within the exciton diffusion range from any donor species and vice versa. Moreover, both the donor and the acceptor phases should form a bicontinuous microphase separated network to allow bipolar charge transport. However, the donor and acceptor molecules are usually incompatible and tend to undergo uncontrolled macrophase separation. To avoid any problems arising from bad contacts at the junction, we have recently shown that the bicontinuous network can be obtained by chemically linking a hole-conducting oligophenylenevinylene (OPV) moiety to an electron-conducting fullerene subunit.[5] The **C_{60}−3PV** hybrid compound has been incorporated in a photovoltaic cell constructed by spin-casting the compound on a glass substrate covered with indium−tin oxide (ITO) and depositing an aluminum film on top. In such a device configuration, the compound is not only able to generate electrons and holes under light irradiation but it also provides pathways for their subsequent collection at opposite electrodes and a photocurrent is obtained. We now report in more detail the preparative procedures used to obtain **C_{60}−3PV** as well as the synthesis of the corresponding higher homologue **C_{60}−4PV**. We also discuss their electrochemical and excited-state properties in solution using the related OPV derivatives **3PV** and **4PV** and the fulleropyrrolidine **FP** as reference compounds. Finally, their incorporation in photovoltaic devices is described.

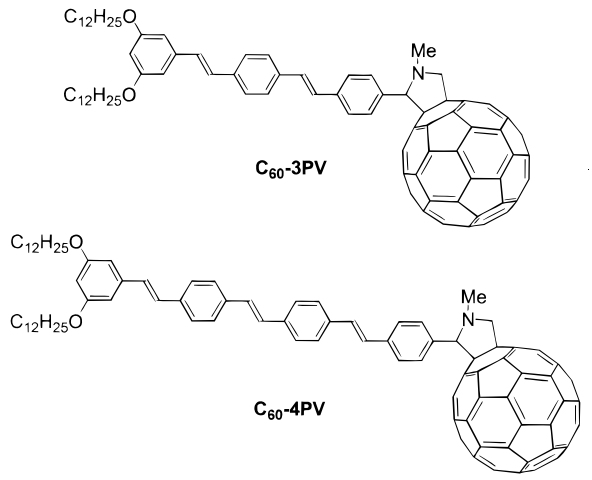

Results and Discussion

Synthesis. The recent progress in the chemistry of C_{60}[6] allows the preparation of many covalent C_{60} derivatives bearing electro- and/or photoactive substituents.[7−10] Some of these systems provided entry into intramolecular processes such as electron or energy transfer, and C_{60} appears to be a particularly interesting electron acceptor in photochemical molecular devices because of its symmetrical shape, its large size, and the properties of its π-electron system.[9] Following the observation of photoinduced electron transfer from conducting oligomers and/or polymers derived from polyphenylenevinylene (PPV) or polythiophene,[4] and the successful preparation of photovoltaic cells from such bulk heterojunction materials,[2,3] a few examples of covalent fullerene derivatives bearing a conjugated oligomer substituent have been synthesized in the past years.[10] As a part of this research, we report here the synthesis of compounds **C_{60}−3PV** and **C_{60}−4PV**. The synthetic approach to prepare those compounds relies upon [3+2] 1,3-dipolar cycloaddition of azomethine ylides to C_{60}.[11] This methodology has proven to be very efficient for the functionalization of C_{60} due to its versatility and the ready availability of the starting materials.[11]

(4) Sariciftci, N. S.; Smilowitz, L.; Heeger, A. J.; Wudl, F. *Science* **1992**, *258*, 1474. Janssen, R. A. J.; Hummelen, J. C.; Lee, K.; Pakbaz, K.; Sariciftci, N. S.; Heeger, A. J.; Wudl, F. *J. Chem. Phys.* **1995**, *103*, 788. Janssen, R. A. J.; Christiaans, M. P. T.; Pakbaz, K.; Moses, D.; Hummelen, J. C.; Sariciftci, N. S. *J. Chem. Phys*. **1995**, *102*, 2628. Kraabel, B.; Hummelen, J. C.; Vacar, D.; Moses, D.; Sariciftci, N. S.; Heeger, A. J.; Wudl, F. *J. Chem. Phys.* **1996**, *104*, 4267. Wang, Y.; Suna, A. *J. Chem. Phys. B* **1997**, *101*, 5627. Pasimeni, L.; Maniero, A. L.; Ruzzi, M.; Prato, M.; Da Ros, T.; Barbarella, G.; Zambianchi, M. *Chem. Commun*. **1999**, 429.

(5) Nierengarten, J.-F.; Eckert, J.-F.; Nicoud, J.-F.; Ouali, L.; Krasnikov, V.; Hadziioannou, G. *Chem. Commun.* **1999**, 617.

(6) Hirsch, A. *The Chemistry of the Fullerenes*; Thieme: Stuttgart, 1994. Diederich, F.; Thilgen, C. *Science* **1996**, *271*, 317. Prato, M. *J. Mater. Chem.* **1997**, *7*, 1097. Diederich, F. *Pure & Appl. Chem*. **1997**, *69*, 395. Diederich, F.; Kessinger, R. *Acc. Chem. Res.* **1999**, *32*, 537.

(7) Reviews related to C_{60}-based donor−acceptor molecular assemblies: Imahori, H.; Sakata, Y. *Adv. Mater*. **1997**, *9*, 537. Martin, N.; Sanchez, L.; Illescas, B.; Perez, I. *Chem. Rev.* **1998**, *98*, 2527. Diederich, F.; Gomez-Lopez, M. *Chem. Soc. Rev.* **1999**, *28*, 263.

(8) For selected examples, see: Khan, S. I.; Oliver, A. M.; Paddon-Row: M. N.; Rubin, Y. *J. Am. Chem. Soc.* **1993**, *115*, 4919. Iyoda, M.; Sultana, F.; Sasaki, S.; Yoshida, M. *Chem. Commun.* **1994**, 1929. Williams, R. M.; Zwier, J. M.; Verhoeven, J. W. *J. Am. Chem. Soc.* **1995**, *117*, 4093. Liddell, P. A.; Sumida, J. P.; Macpherson, A. N.; Noss, L.; Seely, G. R.; Clark, K. N.; Moore, A. L.; Moore, T. A.; Gust, D. *Photochem. Photobiol*. **1994**, *60*, 537. Imahori, H.; Hagiwara, K.; Akiyama, T.; Tanigushi, S.; Okada, T.; Sakata, Y. *Chem. Lett*. **1995**, 265. Drovetskaya, T.; Reed, C. A.; Boyd, P. *Tetrahedron Lett.* **1995**, *44*, 7971. Diederich, F.; Dietrich-Buchecker, C.; Nierengarten, J.-F.; Sauvage, J.-P. *Chem. Commun*. **1995**, 781. Maggini, M.; Dono, A.; Scorrano, G.; Prato, M. *Chem. Commun.* **1995**, 845. Linssen, G.; Dürr, K.; Hanack, M.; Hirsch, A. *Chem. Commun*. **1995**, 103. Diekers, M.; Hirsch, A.; Martin, N.; Sanchez, L.; Seoane, C.; Andreu, R.; Garin, J.; Orduna, J. *Tetrahedron Lett*. **1996**, *37*, 5979. Armspach, D.; Constable, E. C.; Diederich, F.; Housecroft, C.; Nierengarten, J.-F. *Chem. Commun*. **1996**, 2009. Lawson, J. M.; Oliver, A. M.; Rothenfluh, D. F.; An, Y.-Z.; Ellis, G. A.; Ranasinghe, M. G.; Khan, S. I.; Franz, A. G.; Ganapathi, P. S.; Shepard, M. J.; Paddon-Row: M. N.; Rubin, Y. *J. Org. Chem.* **1996**, *61*, 5032. Williams, R. M.; Koeberg, M.; Lawson, J. M.; An, Y.-Z.; Rubin, Y.; Paddon-Row: M. N.; Verhoeven, J. W. *J. Org. Chem*. **1996**, *61*, 5055. Martin, N.; Perez, I.; Sanchez, L.; Seoane, C. *J. Org. Chem.* **1997**, *62*, 5690. Liddell, P. A.; Kuciauskas, D.; Sumida, J. P.; Nash, B.; Nguyen, D.; Moore, A. L.; Moore, T. A.; Gust, D. *J. Am. Chem. Soc*. **1997**, *119*, 1400. Ashton, P. R.; Diederich, F.; Gomez-Lopez, M.; Nierengarten, J.-F.; Preece, J. A.; Raymo, F. M.; Stoddart, J. F. *Angew. Chem., Int. Ed. Engl.* **1997**, *36*, 1448. Safonov, I. G.; Baran, P. S.; Schuster, D. I. *Tetrahedron Lett*. **1997**, *38*, 8133. Kuciauskas, D.; Liddell, P. A.; Moore, A. L.; Moore, T. A.; Gust, D. *J. Am. Chem. Soc*. **1998**, *120*, 10880. Nierengarten, J.-F.; Oswald, L.; Nicoud, J.-F. *Chem. Commun*. **1998**, 1545. Pyo, S.; Rivera, J.; Echegoyen, L. *Eur. J. Org. Chem*. **1998**, 1111. Guldi, D. M.; Torres-Garcia, G.; Mattay, J. *J. Phys. Chem. A* **1998**, *102*, 9679. Gareis, T.; Köthe, O.; Daub, J. *Eur. J. Org. Chem*. **1998**, 1549. Llacay, J.; Veciana, J.; Vidal-Gancedo, J.; Bourdelande, J. L.; Gonzalez-Moreno, R.; Rovira, C. *J. Org. Chem*. **1998**, *63*, 5201. Bourgeois, J.-P.; Diederich, F.; Echegoyen, L.; Nierengarten, J.-F. *Helv. Chim. Acta* **1998**, *81*, 1835. Polese, A.; Mondini, S.; Bianco, A.; Toniolo, C.; Scorrano, G.; Guldi, D. M.; Maggini, M. *J. Am. Chem. Soc*. **1999**, *121*, 3446. Deviprasad, G. R.; Rahman, M. S.; D'Souza, F. *Chem. Commun*. **1999**, 849. Simonsen, K. B.; Konovalov, V. V.; Konovalova, T. A.; Kawai, T.; Cava, M. P.; Kispert, L. D.; Metzger, R. M.; Becher, J. *J. Chem. Soc., Perkin Trans. 2* **1999**, 657. Wedel, M.; Montforts, F.-P. *Tetrahedron Lett*. **1999**, *40*, 7071. Camps, X.; Dietel, E.; Hirsch, A.; Pyo, S.; Echegoyen, L.; Hackbarth, S.; Röder, B. *Chem. Eur. J*. **1999**, *5*, 2362. Nierengarten, J.-F.; Felder, D.; Nicoud, J.-F. *Tetrahedron Lett.* **1999**, *40*, 273.

(9) Imahori, H.; Hagiwara, K.; Aoki, M.; Akiyama, T.; Taniguchi, S.; Okada, T.; Shirakawa, M.; Sakata, Y. *Chem. Phys. Lett*. **1996**, *263*, 545.

(10) (a) Liu, S.-G.; Shu, L.; Rivera, J.; Liu, H.; Raimundo, J.-M.; Roncali, J.; Gorgues, A.; Echegoyen, L. *J. Org. Chem*. **1999**, *64*, 4884. (b) Effenberger, F.; Grube, G. *Synthesis* **1998**, 1372; Segura, J. L.; Martin, N. *Tetrahedron Lett.* **1999**, 3239; Yamashiro, T.; Aso, Y.; Otsubo, T.; Tang, H.; Harima, Y.; Yamashita, K. *Chem. Lett.* **1999**, 443. Knol, J.; Van Hal, P. A.; Langeveld, B. M. W.; Peeters, E.; Janssen, R. A. J.; Hummelen, J. C. presentation at the meeting *Fullerenes'99 − A Workshop on Nanotubes and Fullerene Chemistry*, August 29 − September 2, 1999, Château de Bonas, Castera-Verduzan (France).

(11) Prato, M.; Maggini, M. *Acc. Chem. Res.* **1998**, *31*, 519.

Scheme 1[a]

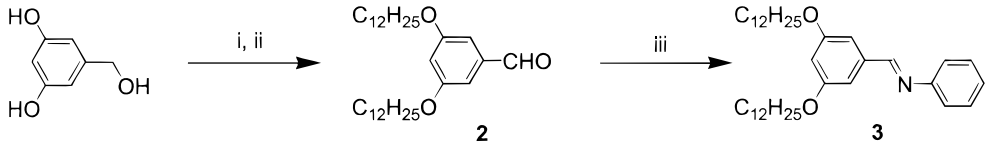

[a] Reagents and conditions: (i) 1-bromododecane, K_2CO_3, DMF, 70 °C, 48 h, 70%; (ii) MnO_2, CH_2Cl_2, rt, 1 h, 90%; (iii) aniline, C_6H_6, reflux, Dean−Stark trap, 24 h, 90%.

Scheme 2[a]

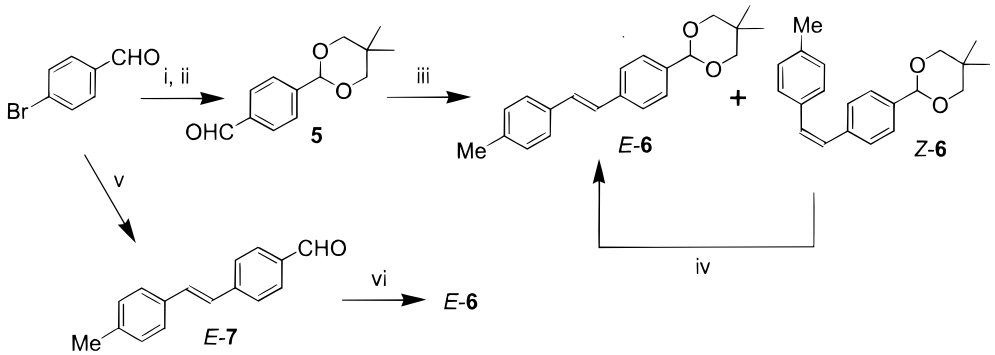

[a] Reagents and conditions: (i) 2,2-dimethylpropane-1,3-diol, *p*-TsOH, C_6H_6, reflux, Dean−Stark trap, 24 h, 95%; (ii) *t*-BuLi, THF, −78 to 0 °C, 1.5 h, then DMF, −78 to 0 °C, 1 h, 98%; (iii) (4-methylbenzyl)triphenylphosphonium chloride, *t*-BuOK, EtOH, rt, 1 h; (iv) I_2, toluene, reflux, 12 h, 70% from **5**; (v) *p*-methylstyrene, $Pd(OAc)_2$, POT, Et_3N, Xylene, 130 °C, 48 h, 70%; (vi) 2,2-dimethylpropane-1,3-diol, *p*-TsOH, C_6H_6, reflux, Dean−Stark trap, 24 h, 95%.

Reaction of 3,5-dihydroxybenzyl alcohol with 1-bromododecane in DMF at 70 °C in the presence of K_2CO_3 yielded **1** in 70% yield (Scheme 1). Subsequent oxidation with MnO_2 in CH_2Cl_2 followed by condensation of the resulting benzaldehyde **2** with aniline in refluxing benzene afforded benzaldimine **3** in an overall 80% yield.

Reaction of *p*-bromobenzaldehyde with 2,2-dimethylpropane-1,3-diol in refluxing benzene in the presence of a catalytic amount of *p*-toluenesulfonic acid (*p*-TsOH) gave the protected aldehyde **4** in 95% yield (Scheme 2). Subsequent treatment with an excess of *t*-BuLi in THF at −78 °C followed by quenching with dry DMF afforded aldehyde **5**. The reaction of **5** with (4-methylbenzyl)triphenylphosphonium chloride in ethanol in the presence of *t*-BuOK under Wittig conditions afforded stilbene **6** as an *E*:*Z* isomer mixture in a 55:45 ratio. The two isomers could be separated by column chromatography and characterized. The isomerization of the *Z* isomer to the *E* was easily achieved by treatment with a catalytic amount of iodine in refluxing toluene. In a preparative procedure, the mixture of isomers obtained from the Wittig reaction was treated without separation with iodine in toluene and the stilbene *E*-**6** was thus obtained in 70% yield. Compound *E*-**6** could also be prepared in two steps from *p*-methylstyrene and *p*-bromobenzaldehyde: a Heck type reaction[12] with $Pd(OAc)_2$ as catalyst in xylene−Et_3N in the presence of tri-*o*-tolylphosphine (POT) and subsequent treatment of the resulting aldehyde *E*-**7** with 2,2-dimethylpropane-1,3-diol gave *E*-**6** in a 65% overall yield.

The preparation of the protected trimer **3PV** was based on the Siegrist reaction (Scheme 3).[13,14] Treatment of stilbene *E*-**6** with benzaldimine **3** in the presence of *t*-BuOK in DMF at 80 °C gave **3PV** in 91% yield. Subsequent deprotection with CF_3CO_2H in CH_2Cl_2/H_2O afforded aldehyde **8**. The 1,3-dipolar cycloaddition[11] of the azomethine ylide generated in situ from **8** and *N*-methylglycine (sarcosine) in refluxing toluene with C_{60} leads to fulleropyrrolidine $\mathbf{C_{60}}$**−3PV** in 43% yield. Thanks to the presence of the two dodecyloxy substituents, compound $\mathbf{C_{60}}$**−3PV** is highly soluble in common organic solvents such as CH_2Cl_2, $CHCl_3$, toluene, or THF, and complete spectroscopic characterization was easily achieved. The ^{1}H NMR spectrum of $\mathbf{C_{60}}$**−3PV** in $CDCl_3$ solution shows all the expected signals. Coupling constants of ca. 17 Hz for the two AB signals corresponding to the two sets of vinylic protons confirmed the *E* stereochemistry of both double bonds of the OPV moiety in $\mathbf{C_{60}}$**−3PV**. Interestingly, the signals corresponding to some of the protons of the pyrrolidine ring and those of the phenyl group directly attached to it are broad at room temperature. A variable-temperature NMR study showed a clear coalescence at ca. 10 °C, and the reversible narrowing of all these peaks shows that a dynamic effect occurs.[15] This indicates restricted rotation of

Scheme 3[a]

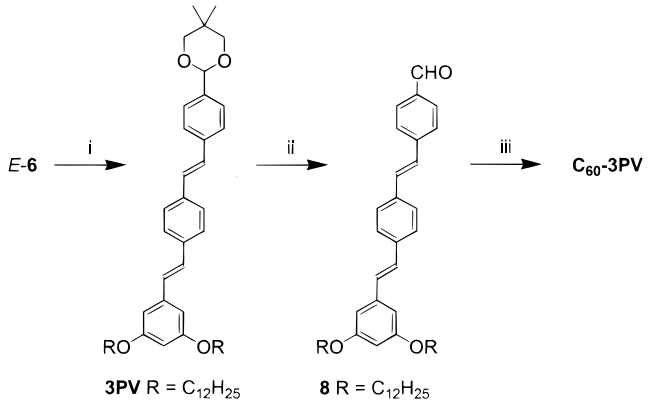

[a] Reagents and conditions: (i) **3**, *t*-BuOK, DMF, 80 °C, 1 h, 91%; (ii) CF_3CO_2H, CH_2Cl_2, H_2O, 5 h, 96%; (iii) C_{60}, sarcosine, toluene, reflux, 16 h, 43%.

(12) Heck, F. H. *Palladium Reagents in Organic Synthesis*; Academic Press: London, 1985.

(13) Siegrist, A. E.; Liechti, P.; Meyer, H. R.; Weber, K. *Helv. Chim. Acta* **1969**, *52*, 2521. Zerban, G.; Meier, H. *Z. Naturforsch. B* **1993**, *48*, 171. Skibniewski, A.; Bluet, G.; Druzé, N.; Riant, O. *Synthesis* **1999**, 459.

(14) For a review on the preparation of OPV derivatives, see: Geerts, Y.; Klärner, G.; Müllen, K. In *Electronic Materials: the Oligomer Approach*; Müllen, K., Wegner, G., Eds.; Wiley-VCH: Weinheim, 1998; pp 1−103.

Scheme 4[a]

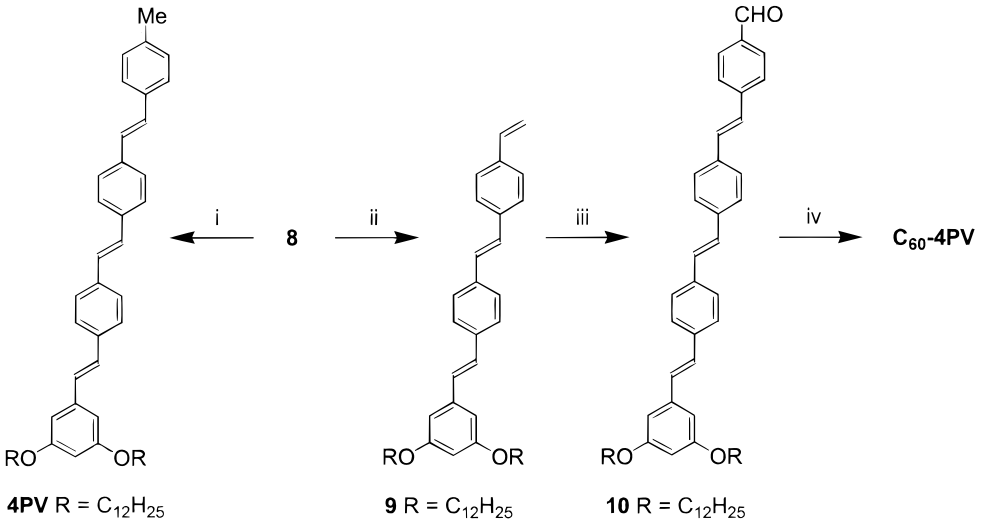

Reagents and conditions: (i) (4-methylbenzyl)triphenylphosphonium chloride, *t*-BuOK, THF, rt, 1 h, then I_2, toluene, reflux, 12 h, 42%; (ii) methyltriphenylphosphonium bromide, *t*-BuOK, THF, rt, 1 h, 82%; (iii) *p*-bromobenzaldehyde, $Pd(OAc)_2$, POT, Et_3N, xylene, 130 °C, 48 h, 60%; (iv) C_{60}, sarcosine, toluene, reflux, 16 h, 40%.

the phenyl substituent on the pyrrolidine ring, and the activation free energy of the rotation was estimated as $\Delta G^{\ddagger} = 13$ kcal mol^{-1} by following the coalescence of the aromatic C−H.[15] This result is in good accordance with the data previously reported by F. Langa and co-workers.[15b] The ^{13}C NMR spectrum of **C_{60}−3PV** is in full agreement with its C_1 symmetry resulting from the presence of the asymmetric C atom in the pyrrolidine ring. The structure of **C_{60}−3PV** is also confirmed by FAB-mass spectroscopy with the molecular ion peak at $m/z = 1426.8$ ($[M + H]^+$, calculated for $C_{109}H_{72}O_2N$: 1426.6). The fragmentation pattern showing peaks at 705.6 and 720.2 corresponding to $[M - C_{60}]^+$ (calculated for $C_{49}H_{71}O_2N$: 705.5) and $[C_{60}]^+$ (calculated: 720.0), respectively, is also consistent with the structure of **C_{60}−3PV**.

Reaction of aldehyde **8** with methyl triphenylphosphonium bromide under Wittig conditions yielded **9** in 82% yield (Scheme 4). Subsequent Heck coupling of **9** with *p*-bromobenzaldehyde with $Pd(OAc)_2$ as catalyst in xylene−Et_3N in the presence of POT gave tetramer **10** in 60% yield. Model compound **4PV** was obtained in 42% yield from the Wittig reaction between aldehyde **8** and (4-methylbenzyl)triphenylphosphonium chloride in THF in the presence of *t*-BuOK followed by treatment with iodine in refluxing toluene. The reaction of C_{60} with **10** in the presence of an excess of sarcosine in refluxing toluene afforded fulleropyrrolidine **C_{60}−4PV** in 40% yield. The ^1H NMR spectrum of **C_{60}−4PV** shows all the expected signals, and the broadening seen in **C_{60}−3PV** for some of the protons of the pyrrolidine ring and those of the phenyl group directly attached to it is also observed for compound **C_{60}−4PV**. The FAB-mass spectrum of **C_{60}−4PV** shows the expected molecular ion peak at 1528.6 (calculated for $C_{117}H_{77}O_2N$: 1528.6) as well as the characteristic peaks at 807.6 ($[M - C_{60}]^+$) and 720.0 ($[C_{60}]^+$) corresponding to the fragmentation.

Model fulleropyrrolidine **FP** was obtained in 42% yield by treatment of C_{60} with benzaldehyde **2** and sarcosine in refluxing toluene (Scheme 5). Restricted rotation of the phenyl substituent on the pyrrolidine ring was also observed for compound **FP**. As in the case of **C_{60}−3PV**, a variable temperature NMR study showed a clear coalescence at ca. 10 °C and the activation free energy of the rotation of the phenyl group was estimated as $\Delta G^{\ddagger} = 13$ kcal mol^{-1}.

Scheme 5[a]

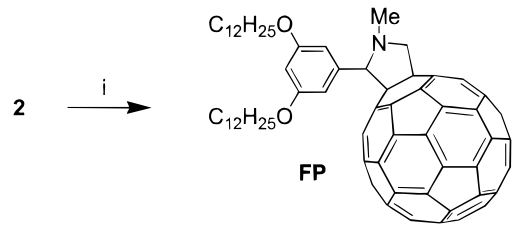

[a] Reagents and conditions: (i) C_{60}, sarcosine, toluene, reflux, 16 h, 42%.

Electrochemistry. The electrochemical properties of compounds **C_{60}−3PV**, **C_{60}−4PV**, **3PV**, **4PV**, and **FP** were investigated by cyclic voltammetry (CV) and/or by Osteryoung square wave voltammetry (OSWV). All the experiments were performed at room temperature in *o*-dichorobenzene solutions, containing tetra-*n*-butylammonium hexafluorophosphate (0.05 M) as supporting electrolyte, with a glassy carbon as the working electrode, a Pt wire as counter electrode, and a Ag/AgCl as the reference electrode. Potential data for all of the compounds are collected in Table 1.

The fullerene−OPV derivatives **C_{60}−3PV** and **C_{60}−4PV** show three reversible reduction peaks in the cathodic scan. A chemically irreversible oxidation peak is observed in the anodic scan for fulleropyrrolidine **C_{60}−3PV**. As shown by the comparison with model compounds **3PV** and **FP**, the OPV and fulleropyrrolidine oxidation waves cannot be clearly distinguished because both constituents are oxidized at similar potentials. By comparing the results of fulleropyrrolidine **C_{60}−4PV** with those of the model compound **4PV**, the first irreversible oxidation peak observed for **C_{60}−4PV** at 1.193 V vs Ag/AgCl is assigned to the OPV moiety. The second oxidation of the OPV addend cannot be clearly distinguished from the fulleropyrrolidine oxidation. In the case of the OPV model compounds **3PV** and **4PV**, it was not possible to detect any reduction waves using CV. All of the C_{60} derivatives (**FP**, **C_{60}−3PV**, and **C_{60}−4PV)** essentially retain the cathodic electrochemical pattern of the parent fullerene but the reduction potentials of all of these species are shifted to more negative

(15) (a) Günther, H. *NMR-Spektroskopie*, 2nd ed.; Thieme: Stuttgart, 1983. (b) De la Cruz, P.; De la Hoz, A.; Font, L. M.; Langa, F.; Perez-Rodriguez, M. C. *Tetrahedron Lett.* **1998**, *39*, 6053.

Table 1. Electrochemical Properties of C_{60} and Compounds **C_{60}−3PV**, **C_{60}−4PV**, **3PV**, **4PV,** and **FP**[a]

	E_{red}^1	E_{red}^2	E_{red}^3	E_{red}^4	E_{ox}^1	E_{ox}^2
C_{60}	−0.552 (76)	−0.928 (71)	−1.363 (68)	−1.820 (65)		
FP	−0.643 (41)	−1.009 (40)	−1.520 (40)	−1.965[b]	+1.389[c]	+1.550[c]
3PV	−2.005[b]				+1.305[c]	+1.520[c]
4PV	−1.956[b]				+1.156[c]	+1.440[c]
C_{60}−3PV	−0.654 (64)	−1.019 (64)	−1.534 (54)	−1.947[b]	+1.354[c]	
C_{60}−4PV	−0.665 (55)	−1.029 (62)	−1.552 (68)	−1.865[b]	+1.193[c]	+1.390[c]

[a] CV measurements in *o*-dichlorobenzene; *n*-Bu_4PF_6 (0.05 M) as supporting electrolyte; glassy carbon as working electrode; Pt wire as counter electrode; Ag/AgCl as reference electrode; scan rate 0.1 V s^{-1}; $E_{1/2} = (E_{ox} + E_{red})/2$ (in V vs Ag/AgCl); data shown in parentheses are ΔE_p values in mV. [b] Determined by OSWV technique. [c] Irreversible process, peak potentials.

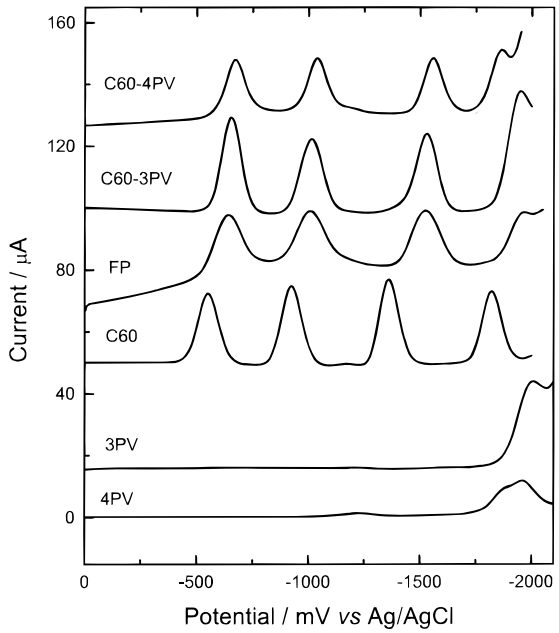

Figure 1. OSWVs of C_{60}, **FP**, **C_{60}−3PV**, **C_{60}−4PV**, **3PV**, and **4PV** on GC electrode in *o*-dichlorobenzene solution at room temperature.

values when compared to those of pure C_{60}. This is the classical behavior observed for most fullerene derivatives, whose cyclic voltammograms are typically characterized by small shifts to more negative potentials as the saturation of a double bond on the C_{60} surfaces causes a partial loss of "conjugation".[16] Comparison of the reduction potentials of **C_{60}−3PV** and **C_{60}−4PV** with those of model compound **FP** shows a small but evident trend. The first three reduction potentials of both **C_{60}−3PV** and **C_{60}−4PV** are slightly shifted to more negative values by 10−14 and 20−32 mV, respectively. In contrast, a slight positive shift was observed for the OPV-based oxidations of both **C_{60}−3PV** and **C_{60}−4PV** by about 40 mV with respect to the corresponding OPV model compounds. These shifts must be a consequence of small electronic interactions between the donating OPV moiety and the accepting C_{60} spheroid, resulting in a more difficult oxidation for the OPV group and a more difficult reduction for the C_{60} moiety. This is in good agreement with the results recently reported for ferrocenyl fulleropyrrolidines[17] and for dimethylaniline-substituted dithienylethyl fulleropyrrolidines.[10a]

While CV experiments were unable to detect a fourth reduction wave for **C_{60}−3PV** and **C_{60}−4PV** and no reduction processes at all for **3PV** and **4PV**, OSWV revealed such processes easily (Figure 1).

To try to assign these fourth reduction processes as either fullerene- or donor-based, their potentials were carefully compared with those observed for **3PV** and **4PV** under identical conditions (Figure 1). The reductions observed for **3PV** and **4PV** occur at −2.005 and −1.956 V, respectively. On the basis of the results observed for **FP** (fourth reduction at −1.965 V) and for **4PV** and on the expectation that the fourth reduction of **C_{60}−4PV** would be cathodically shifted (as the first three are), we feel that the −1.865 V fourth reduction is probably OPV-based. In the case of **C_{60}−3PV**, the situation is not as clear and the fourth reduction process probably contains contributions from both C_{60} and OPV moieties, although it is impossible to establish this unequivocally on the basis of the current data. If these assignments are correct, it is interesting to note that the OPV-based reductions for **C_{60}−3PV** and **C_{60}−4PV** are anodically shifted by 58 and 91 mV, respectively, compared with those of the models **3PV** and **4PV**. This is consistent with the positive shift observed for the OPV-based oxidations due to the electronic interactions between the donating substituted OPV moiety and the accepting C_{60} spheroid as discussed above.

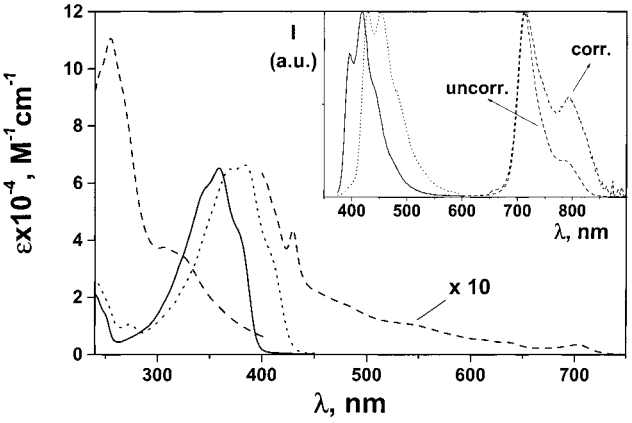

Figure 2. Absorption and (inset) normalized luminescence spectra of the reference compounds **3PV** (full line), **4PV** (dotted line), and **FP** (dashed line) in CH_2Cl_2 at 298 K. The absorption spectrum of **FP** is multiplied by a factor of 10 above 400 nm. In the inset, the luminescence spectrum of **FP** corrected for the detector response is also reported; no correction is required in the spectral region of the OPV derivatives.

Photophysical Properties. The electronic absorption spectra of the reference compounds **3PV**, **4PV**, and **FP** in CH_2Cl_2 solution are reported in Figure 2. The absorption band of the less extended π-conjugated **3PV** system lies at a higher energy relative to **4PV** but, interestingly, the molar extinction coefficients are quite comparable in the two cases; these spectra closely resemble those of previously reported unsubstituted oligostyrylarenes in ethanol solution.[18] The absorption spectrum of the fulleropyrrolidine derivative **FP** in CH_2Cl_2 displays two very intense bands in the UV and much weaker features in the vis spectral region (Table 2). In particular, two band maxima attributable to the lowest (λ_{max} = 704 nm) and lowest *allowed*

(16) Echegoyen, L.; Echegoyen, L. E. *Acc. Chem. Res.* **1998**, *31*, 593.
(17) Maggini, M.; Karlsson, A.; Scorrano, G.; Sandona, G.; Farnia, G.; Prato, M. *Chem. Commun.* **1994**, 589.
(18) Meier, H. *Angew. Chem., Int. Ed. Eng.* **1992**, *31*, 1399.

Table 2. Electronic Absorption and Luminescence Data in CH_2Cl_2[a]

	absorption	luminescence			
	293 K	293 K			77 K
	λ_{max} ($\epsilon \times 10^{-3}$) nm (M^{-1} cm^{-1})	λ_{max}, nm	τ,[b] ns	Φ_{em}	λ_{max}, nm
FP	255 (110); 305 (37.5) 430 (4.4); 704 (0.3)	710	1.3	0.00055	722
3PV	359 (65.2)	396	1.0	1.00	402
4PV	383 (66.0)	428	1.0	0.66	434
C_{60}−3PV	253 (89.0); 348 (57.7); 360 (57.5); 430 (4.6); 702 (0.3)	710	1.2	0.00055	720
C_{60}−4PV	254 (123); 388 (99.1) 702 (0.3)	710	1.2	0.00055	718

[a] For **3PV** and **4PV** the fluorescence spectra and quantum yields were obtained upon excitation on their absorption maxima; for OPV's such experimental data can be dependent on the excitation wavelength due to the presence of different rotamers (see ref 19). For **FP**, **C_{60}−3PV**, and **C_{60}−4PV** the fluorescence spectra and quantum yield values are independent from the excitation wavelength. [b] λ_{exc} = 337 nm (see Experimental Section).

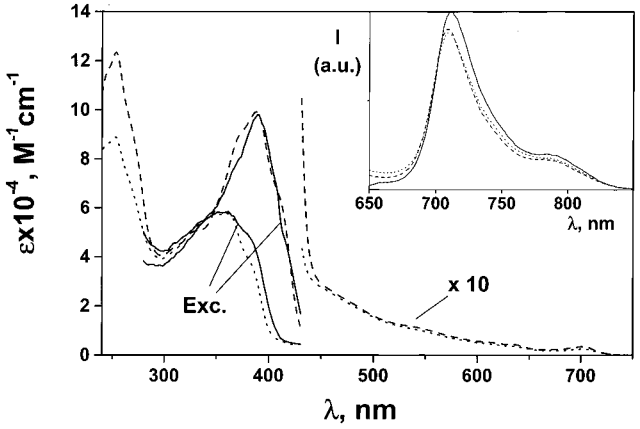

Figure 3. Absorption spectra of **C_{60}−3PV** (dotted line) and **C_{60}−4PV** (dashed line) in CH_2Cl_2 at 298 K; above 430 nm they are multiplied by a factor of 10. The full line is the corrected excitation spectra taken at λ_{em} = 710 nm (maximum of the fullerene moiety fluorescence). Inset: fluorescence spectra of **C_{60}−3PV** (dotted line) and **C_{60}−4PV** (dashed line) upon preferential excitation of the phenylenevinylene moiety, namely 360 and 385 nm respectively; the full line represents the normalized spectrum of **FP**, and can be quantitatively compared to the other spectra; for more details see text.

(λ_{max} = 430 nm) singlet transitions are observed. The absorption spectrum of **FP** is very similar to that of the simpler *N*-methylfulleropyrrolidine, which was earlier reported in toluene solution,[11] thus showing modest perturbations induced by the phenylene fragment bound to the pyrrolidine ring.

The absorption spectra of the two-component systems **C_{60}−3PV** and **C_{60}−4PV** are reported in Figure 3. A comparison with the profiles obtained upon addition of the spectra of the relative component units shows some significant differences. Plain superimposition is observed only above 500 nm, whereas between 400 and 450 nm the experimental spectra are broader. In the UV portion, particularly in the 300−400 nm region, the largest differences are found, with the spectrum of **C_{60}−3PV** being 20% less intense than the sum of its components and that for **C_{60}−4PV** being 25% more intense. At first sight, these results could suggest significant ground-state interactions between the two chromophores, somehow in contrast with the above-mentioned similarity between the spectrum of **FP** and that of plain *N*-methylfulleropyrrolidine. However, it is conceivable that the two σ bonds connecting the OPV's and the fullerene lead to a relatively good degree of electronic insulation. Therefore, we tend to attribute the differences between the absorption spectra of **C_{60}−3PV** and **C_{60}−4PV** with the sum of their component units to a peculiar rotameric equilibrium[19] within the OPV moieties in the arrays, also brought about by the cumbersome fullerene fragment. In this regard it is worth pointing out that differences are substantially found only in the spectral absorption region of the OPV fragments. On the other hand, scarce electronic interaction is argued also from the electrochemical properties.

The fluorescence spectra of the reference compounds **3PV**, **4PV**, and **FP** in CH_2Cl_2 solution at 298 K are reported in the inset of Figure 2**.** In a CH_2Cl_2 rigid matrix at 77 K, the spectra of the two OPV's are more resolved and red shifted relative to 298 K, whereas the luminescence decay at λ_{em} = 470 nm is biexponential for **3PV** (τ_1 = 1.0 ns and τ_2 = 6.9 ns) and monoexponential for **4PV** (τ = 0.8 ns). This behavior can be rationalized on the basis of a different rotameric equilibrium in the rigid matrix for the two OPV's.[19]

3PV and **4PV** are potent fluorophores, as expected for OPV systems especially in nonpolar solvents,[18,20] displaying quantum yields of 1.00 and 0.66 at 298 K respectively and an excited-state lifetime of 1.0 ns in both cases. Thus, radiationless paths contribute to the deactivation of the singlet excited state of **4PV** but not of **3PV**. This different behavior can be due to various factors.[21] For **4PV**, a more extended π-system results in a lower level for the energy of the singlet excited state, which is expected to favor radiationless processes (energy-gap law).[22] Likewise, the more extended geometric relaxations expected for the case of **4PV** may promote radiationless processes.[23] Elsewhere it has been reported that remarkable variations of the emission quantum yields are observed by changing the substituents (or simply their location) on the OPV skeleton,[20,23] but this cannot be clearly invoked in the present case. Any attempt to detect phosphorescence from the lowest triplet excited state of **4PV** (also by eliminating the prompt fluorescence by time gated techniques) gave no result, as typically observed for OPV derivatives.[18,24]

FP exhibits a fluorescence band with λ_{max} = 710 nm; its emission quantum yield and excited-state lifetime (Φ_{em} = 0.00055, τ = 1.3 ns) are, respectively, slightly higher and remarkably shorter relative to those of methanofullerenes in CH_2Cl_2 solution,[24] which implies a higher radiative rate constant k_r ($k_r = \Phi_{em}/\tau$). The location of the emission band maximum is negligibly affected in the corrected spectrum (Figure 2, inset). The excited-state lifetime (identical to plain C_{60} and shorter than

(19) Mazzuccato, U.; Momicchioli, F. *Chem. Rev.* **1991**, *91*, 1679.

(20) Strehmel, B.; Sarker, A. M.; Malpert, J. H.; Strehmel, V.; Seifert, H.; Neckers, D. G. *J. Am. Chem. Soc.* **1999**, *121*, 1226

(21) Birks, J. R. *Photophysics of Aromatic Molecules*; Wiley-Interscience: London, U.K., 1969; Chapter 5.

(22) (a) Englman, R.; Jortner, J.; *Mol. Phys.* **1970**, *18*, 145. (b) Freed, K.; Jortner, J. *J. Chem. Phys.* **1970**, *52*, 6272.

(23) Van Hutten, P. F.; Krasnikov, V. V.; Hadziioannou, G. *Acc. Chem. Res.* **1999**, *32*, 257.

(24) Beljonne, D.; Cornil, J.; Brédas, J. L.; Friend, R. H. *Synth. Met.* **1996**, *76*, 61.

methanofullerenes)[25] is identical to that reported for several *N*-methylfulleropyrrolidines in methycyclohexane,[26] benzene,[27a] and toluene.[27b] The excitation spectrum of **FP** taken at $\lambda_{em} =$ 710 matches the corresponding absorption profile throughout the UV−vis spectral region, indicating that the lowest singlet ($^1\pi\pi^*$) excited state is populated with the same (presumably unitary) efficiency from the upper lying levels. In the rigid matrix at 77 K, the fluorescence band of **FP** is shifted to 722 nm, whereas no phosphorescence could be detected, as usually happens for fullerene compounds under these conditions.[25]

Upon excitation of **C$_{60}$−3PV** and **C$_{60}$−4PV** in correspondence to the absorption maxima of the OPV fragments, i.e., 360 and 385 nm, no trace of OPV fluorescence is detected both at 298 and 77 K, under experimental conditions identical to those for the detection of the fluorescence of the OPV's reference compounds. In practice, this means that the luminescence intensity is, if any, less than 1000 times that of the reference compounds. Accordingly, the quenching process of the OPV singlet is expected to occur within 1 ps or less, since the singlet lifetime of the OPV's is 1.0 ns (Table 2). Unfortunately such time scale is well above the resolution of our instrumentation (20 ps).

The fullerene moiety fluorescence is, conversely, still observed. Upon excitation of **FP**, **C$_{60}$−3PV** and **C$_{60}$−4PV** at 550 nm, where only the fullerene fragment absorbs, the emission quantum yields at 298 K are identical (5.5×10^{-4}) within the experimental uncertainty. More importantly, such quantum yield values are also obtained upon UV excitation on the absorption maxima of the OPV fragments (i.e., 360 and 385 nm, see above). As pointed out in the discussion of the absorption spectra, in the UV region it is not possible to sort out accurately the amount of light absorbed by each component in **C$_{60}$−3PV** and **C$_{60}$−4PV**; however one can safely assert that at least 60% of the light at respectively 360 and 385 nm is addressed to the OPV fragment. Therefore, our results are consistent with the sensitization of the fullerene fluorescence, thus indicating that in CH_2Cl_2 a OPV → C_{60} photoinduced energy-transfer process occurs. This is confirmed by the corrected excitation spectra (Figure 3) that are very well matched with the absorption profiles in the 300−430 nm region where, with alternating prevalence (see Figure 2), both the OPV and the fullerene fragments absorb. Switching to the more polar benzonitrile solvent does not change the result. Again, under these conditions, emission and excitation spectra indicate that photoinduced energy transfer is the only intercomponent process, at least within the experimental uncertainty.[28]

By using the luminescence data of the fragments which act as energy donors (**3PV** and **4PV**) and the absorption spectrum of the acceptor, **FP**, it is possible to draw some conclusions regarding the type of energy transfer mechanism that is operative in our cases. Two mechanisms, the dipole−dipole (Förster)[29] or the double electron exchange (Dexter),[30] may be involved. The possible contribution by the dipole−dipole energy transfer, which is pertinent to singlet−singlet interaction schemes, can be evaluated on the basis of the following equations:

$$k_{en}{}^{F} = \frac{1}{\tau}\left(\frac{R_c}{d}\right)^6 \quad (1)$$

$$R_c{}^6 = \frac{9000(\ln 10)K^2\Phi}{128\pi^5 N n^4} J_F \quad (2)$$

These allow us to obtain estimates for (i) the energy transfer rate constant, $k_{en}{}^{F}$, and (ii) the critical transfer radius, R_c, i.e., the distance between the fragments for which $k_{en}{}^{F}$ equalizes the intrinsic deactivation of the donor, $k_d = \tau^{-1}$. In eqs 1 and 2, Φ and τ are the luminescence quantum yield and lifetime of the donor fragments, **3PV** and **4PV** (Table 2), $J_F = \int F(\bar{\nu})\epsilon(\bar{\nu})/\bar{\nu}^4 d\bar{\nu} / \int F(\bar{\nu})\, d\bar{\nu}$ is the overlap integral between the luminescence spectrum on an energy scale (cm^{-1}) of the donor ($F(\bar{\nu})$ of **3PV** or **4PV**) and the absorption spectrum of the acceptor ($\epsilon(\bar{\nu})$ of **FP**); J_F is 1.4×10^{-14} and 1.1×10^{-14} cm^6 mol^{-1} for the **3PV** and **4PV** cases, respectively; K^2 is a geometric factor (tentatively taken as $^2/_3$), $N = 6.02 \times 10^{23}$ mol^{-1}, and n is the refractive index of the solvent. Calculations provided $R_c = 35.3$ and 31.6 Å for the couples **3PV**/**FP** and **4PV**/**FP**, respectively, and $k_{en}{}^{F} > 10^{12}$ s^{-1} for $d \leq 10$ Å in both cases.

It should be pointed out that these findings are appropriate for a two-center system whose donating and accepting components retain their electronic identity.[31] However, since from the absorption spectra this cannot be assumed for granted (see above), the alternative mechanism for energy transfer, the double-electron exchange Dexter-type transfer, should also be considered.[30] This latter mechanism requires a certain amount of through-bond electronic communication (represented by the electronic coupling term H, see below) and is usually found to be important for triplet−triplet transfers.

We have performed model calculations according to the Dexter approach by evaluating the pertinent spectral overlap, J_D, equations (eqs 3−5), with $J_D = 1.4 \times 10^{-4}$ and 8.0×10^{-5} cm for the **3PV** and **4PV** cases, respectively. Estimates of $k_{en}{}^{D}$ were obtained for H_o values ranging from 10 to 100 cm^{-1}, which correspond to moderately coupled moieties,[32] and by assuming an attenuation factor $\beta = 0.1$ $Å^{-1}$.[33] d_o values ranging from 3 to 10 Å were employed, roughly corresponding to side-to-side and center-to-center geometries, respectively.

$$J_D = \frac{\int F(\bar{\nu})\epsilon(\bar{\nu})\, d(\bar{\nu})}{\int F(\bar{\nu})\, d\bar{\nu} \int \epsilon(\bar{\nu})\, d\bar{\nu}} \quad (3)$$

$$k_{en}{}^{D} = \frac{4\pi^2 H^2}{h} J_D \quad (4)$$

$$H = H_o \exp[-0.5\beta(d - d_o)] \quad (5)$$

We found that the Förster mechanism is mostly effective up to $d =$ 15 to 20 Å and that an interplay of the two energy transfer mechanisms can only be operative for longer distances or for larger H values; at any rate, energy transfer is always found to predominate over intrinsic deactivation, $k_{en} \gg k_d$ ($k_{en} = k_{en}{}^{F} +$

(25) Armaroli, N.; Diederich, F.; Dietrich-Buchecker, C. O.; Flamigni, L.; Marconi, G.; Nierengarten, J.-F.; Sauvage, J.-P. *Chem. Eur. J.* **1998**, *4*, 406.

(26) Guldi, D. M.; Maggini, M.; Scorrano, G.; Prato, M. *J. Am. Chem. Soc.* **1997**, *119*, 974.

(27) Kuciauskas, D.; Lin, S.; Seely, G. R.; Moore, A. L.; Moore, T. A.; Gust, D. *J. Phys. Chem.* **1996**, *100*, 15926. (b) Luo, C.; Fujitsuka, M.; Watanabe, A.; Ito, O.; Gan, L.; Huang, Y.; Huang, C.-H. *J. Chem. Soc., Faraday Trans*. **1998**, *94*, 527.

(28) Armaroli, N.; Barigelletti, F.; Ceroni, P.; Eckert, J.-F.; Nicoud, J.-F.; Nierengarten, J.-F. *Chem. Commun.* **2000**, 599.

(29) Förster, T. *Discuss. Faraday Soc*. **1959**, *27*, 7.

(30) Dexter, D. L. *J. Chem. Phys*. **1953**, *21*, 836.

(31) Balzani, V.; Scandola, F. *Supramolecular Photochemistry*; Ellis Horwood: Chichester, U.K.. 1991; Chapter 3.

(32) (a) Förster, Th. In *Modern Quantum Chemistry*; Sinaoglu, O., Ed.; Academic Press: New York, 1965; Vol. 111, p 93. (b) Kavarnos, G. J. In *Fundamentals of Photoinduced Electron Transfer*; VCH Publishers: New York, 1993; Chapter 6.

(33) Harriman, A.; Ziessel, R. *Chem. Commun.* **1996**, 1707.

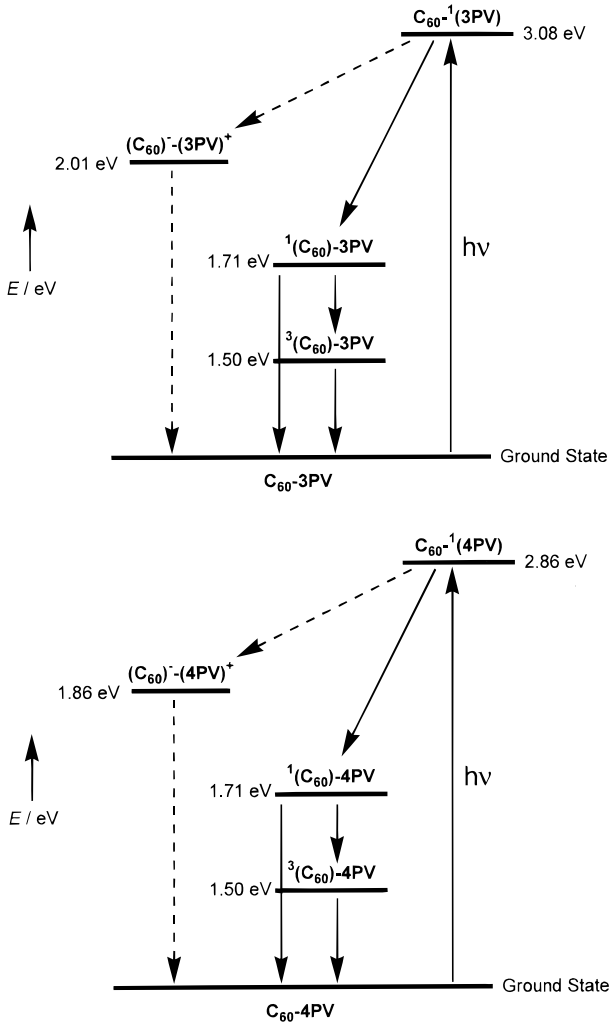

Figure 4. Energy-level diagrams describing the excited-state deactivation pathways and the intercomponent energy transfer processes for C_{60}−**3PV** (top) and C_{60}−**4PV** (bottom) in CH_2Cl_2 solutions.

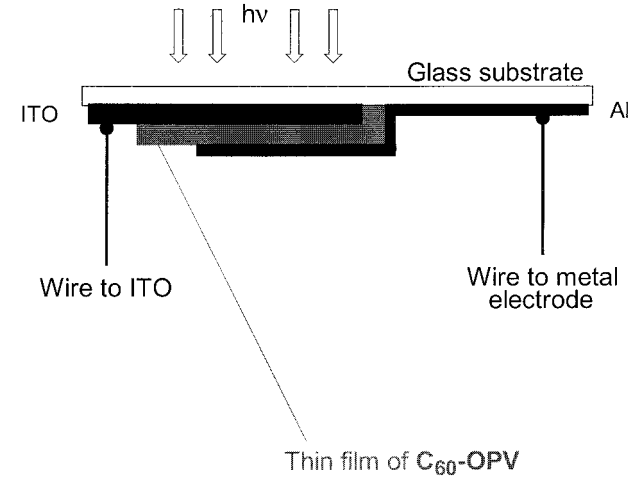

Figure 5. Schematic structure of the photovoltaic cell.

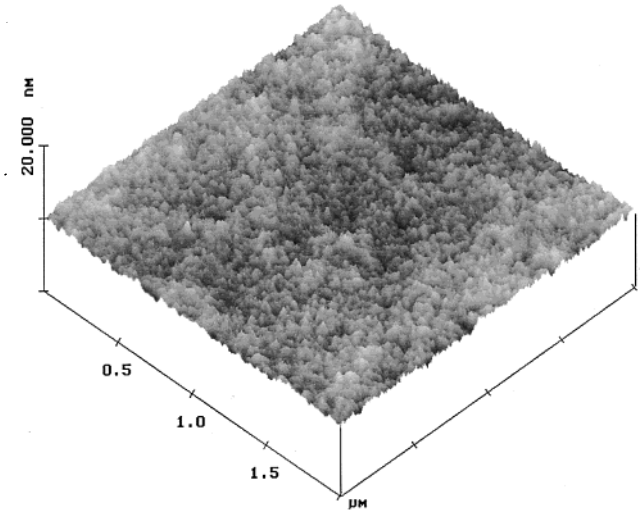

Figure 6. AFM image (tapping mode) showing the topography of a spin coated C_{60}−**3PV** film on mica.

k_{en}^{D}), and the sensitization step is expected to be quantitative (efficiency > 90%) up to $d = 30$ Å.

From the electrochemical data[34] one can locate the energy position of the charge separated states C_{60}^{-}−**3PV**$^{+}$ and C_{60}^{-}−**4PV**$^{+}$ at 2.01 and 1.86 eV, respectively. The energy position of the lowest singlet excited states of the **3PV** and **4PV** fragments can be estimated at 3.08 and 2.86 eV, corresponding to the peak of highest energy feature in the 77 K fluorescence spectra. Consequently, in principle, at 298 K photoinduced electron transfer could also occur from the lowest excited singlet state in CH_2Cl_2 solution, but apparently it does not take place. Of course, given the experimental uncertainty on the emission quantum yields and corrected excitation spectra, we cannot completely rule out a (minor) occurrence of electron transfer but, if any, this is by far negligible relative to energy transfer, i.e., definitely below a 10% efficiency. Finally, no quenching of the fullerene lowest singlet excited state is observed; this is consistent with its low energy content (1.71 eV) which makes impossible both energy and electron transfer quenching (see above). No quenching can be expected also for the lowest fullerene triplet state which is expected to be even lower-lying (Figure 4), typically around 1.50 eV, as determined by theoretical calculations for some fullerene derivatives.[26,35] Indeed, the triplet lifetime is found to be unaffected in passing from **FP** to **3PV** and **4PV**, i.e. 540 ns and 31 μs in air-equilibrated and deoxygenated solution, respectively.

Incorporation in Photovoltaic Cells. The photovoltaic devices (Figure 5) consist of a metal (Al) contact on the surface of an organic film of the C_{60}−**OPV** derivative on a partially coated ITO glass. The organic layer was prepared by spin coating from chloroform solutions. The surface morphology of C_{60}−**3PV** and C_{60}−**4PV** spin-coated on a solid substrate (mica) have been studied by atomic force microscopy (AFM). The AFM image obtained for a film of C_{60}−**3PV** is shown in Figure 6 and reveals a continuous film with small roughness. The films obtained from C_{60}−**4PV** show a similar surface morphology.

The current−voltage characteristics of ITO/C_{60}−**3PV**/Al devices in dark and under illumination, at $\lambda = 400$ nm with an intensity of 12 mW/cm^2, are depicted in Figure 7. Forward bias is defined as positive voltage applied to the ITO electrode. It is known[36] that C_{60} can form "quasi-ohmic" contacts with Al and ITO electrodes. Therefore, the relatively high absolute value of the dark current especially in reverse bias (Figure 7) may be attributed to a continuous phase of C_{60} between the electrodes. Under illumination, the short-circuit current density and the open-circuit voltage are about 10 μA/cm^2 and 0.46 V, respectively. The photosensitivity of this device at zero bias is about

(34) See ref 30, p 44.

(35) Armaroli, N.; Diederich, F.; Echegoyen, L.; Habicher, T.; Flamigni, L.; Marconi, G.; Nierengarten, J.-F. *New J. Chem.* **1999**, *23*, 77.

(36) Yonehara, H.; Pac, C. *Appl. Phys. Lett.* **1992**, *61*, 575.

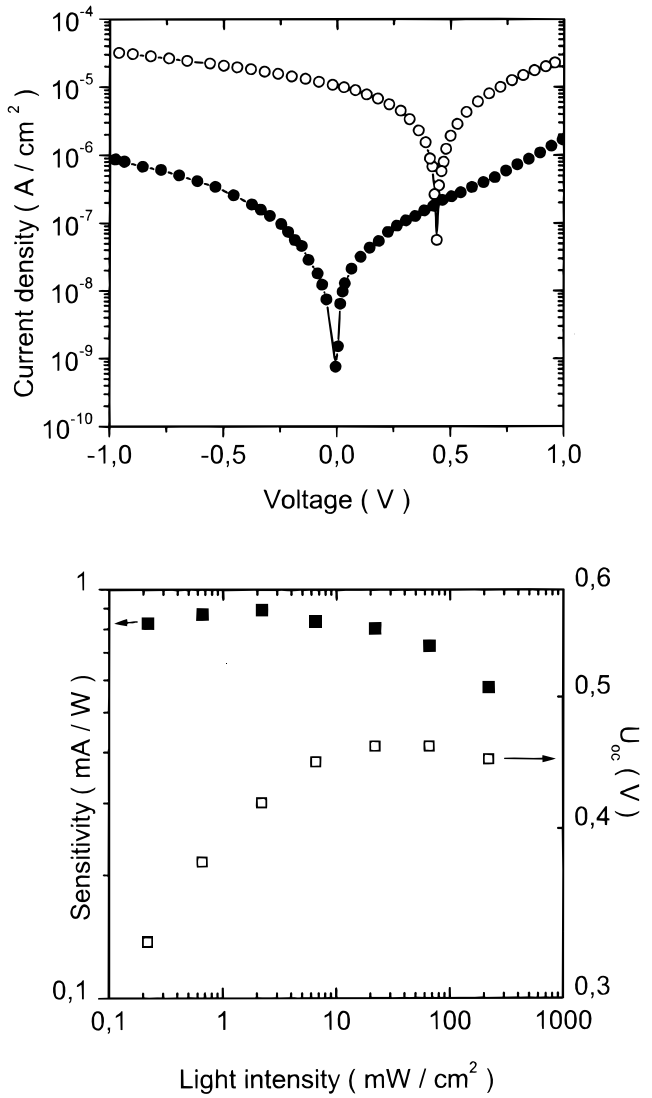

Figure 7. (top) Current−voltage characteristics for the ITO/**C_{60}−3PV**(140 nm)/Al device in the dark (solid circles) and under illumination at $\lambda = 400$ nm with an intensity of 12 mW/cm^2 (open circles). (bottom) The dependence of photosensitivity (solid squares) and open-circuit voltage (open squares) of the ITO/**C_{60}−3PV**/Al device on incident light intensity.

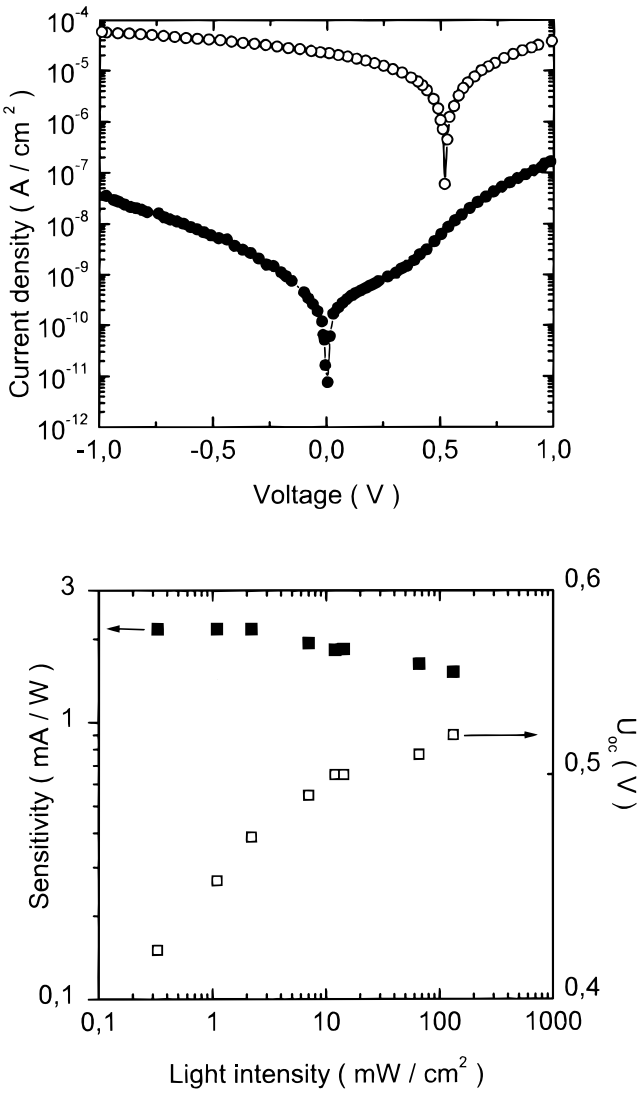

Figure 8. (top) Current−voltage characteristics for the ITO/**C_{60}−4PV**(120 nm)/Al device in the dark (solid circles) and under illumination at $\lambda = 400$ nm with an intensity of 12 mW/cm^2 (open circles). (bottom) The dependence of photosensitivity (solid squares) and open-circuit voltage (open squares) of the ITO/**C_{60}−4PV**/Al device on incident light intensity.

0.8 mA/W. The fill-factor, a measure of the squareness of the I−V characteristic, is equal to 0.3. Figure 7b shows the variation of the sensitivity and the open-circuit voltage as a function of the intensity of light. We observe saturation of the open-circuit voltage at about 0.45 V. This value is quite typical for the interpenetrating blends sandwiched between Al and ITO and roughly corresponds to the difference of their work functions. The sensitivity shows a decrease with increasing light intensity above 10 mW/cm^2.

The current−voltage characteristics of ITO/**C_{60}−4PV**/Al devices in the dark and under illumination, at $\lambda = 400$ nm with an intensity of 12 mW/cm^2, are presented in Figure 8. Similar to the ITO/**C_{60}−3PV**/Al device, the ITO/**C_{60}−4PV**/Al one shows almost symmetrical I−V characteristics in the dark. The photovoltaic characteristics of the ITO/**C_{60}−4PV**/Al device at zero bias are quite similar to those of the one obtained from **C_{60}−3PV**. An increase in the photosensitivity (2.2 mA/W) occurs with a slight increase in the open-circuit voltage (0.52 V).

The monochromatic power conversion efficiency of the ITO/**C_{60}−3PV**/Al and ITO/**C_{60}−4PV**/Al devices are equal to 0.01% and 0.03%, respectively. It is noteworthy that in the case of solar cells made of pure OPV films sandwiched between Al and ITO electrodes, photovoltaic sensitivities and monochromatic energy conversion are typically smaller by 2 orders of magnitude.[4] However, the performances of the ITO/**C_{60}−3PV**/Al and ITO/**C_{60}−4PV**/Al devices are not as good as that observed for some PPV-based solar cells which consist of bicontinuous networks of internal donor−acceptor heterojunctions. We believe that this lower efficiency could result from the low contribution of the photoinduced electron transfer from the OPV moiety excited state to the C_{60} sphere as evidenced in solution by the photophysical investigations. Effectively, the main part of the light energy absorbed by the OPV moieties is conveyed to the fullerene by energy transfer and, since electron transfer from the fullerene lowest singlet excited state is not possible due to its low energy content (Figure 4), electron/hole pairs could not be generated anymore. Thus, only a small part of the absorbed light is able to contribute effectively to the photocurrent. In addition, the fact that no photovoltaic effect could be detected in the spectral region where only the fullerene unit absorbs is also totally consistent with the results of the

photophysical studies. This latest observation is also important since it shows that the electron injection from the fullerene singlet excited state into the ITO electrode cannot result in an effective photocurrent. Therefore, the photovoltaic effect detected in our solar cells when light energy is absorbed by the OPV subunits can also not be the result of a photosensitization effect from the OPV to the fullerene. Thus, as outlined before, the photocurrent must be the result of a photoinduced electron transfer from the OPV moieties excited state to the C_{60} spheres followed by electron injection from the resulting fullerene radical anions into one electrode and a hole injection from the resulting OPV radical cations into the other electrode. For both ITO/**C$_{60}$−3PV**/Al and ITO/**C$_{60}$−4PV**/Al devices, the absolute magnitude of the dark current, the photosensitivity, and the open-circuit voltage depend strongly on the device thickness. It should be mentioned also that we use Al as a metal electrode. Typically, the open-circuit voltage and the short-circuit current of organic photovoltaic cells are significantly better when Ca is used instead of Al.[2]

Conclusions

Fulleropyrolidine derivatives functionalized with OPV subunits have been synthesized and both electrochemical and photophysical studies in solution have revealed that there are small electronic ground-state interactions between the covalently bonded OPV moiety and the fullerene sphere in **C$_{60}$−3PV** and **C$_{60}$−4PV**. The photophysical investigations have shown that, in fluid solution (polar and apolar), an efficient singlet−singlet OPV → C_{60} photoinduced energy transfer occurs whereas electron transfer, if any, is a minor process. Photovoltaic cells have been prepared from both **C$_{60}$−3PV** and **C$_{60}$−4PV**. A photocurrent has been observed for both ITO/**C$_{60}$−3PV**/Al and ITO/**C$_{60}$−4PV**/Al devices showing that photoinduced electron transfer does take place. The results obtained in fluid solution and in the photovoltaic devices seem to be contradictory. However, one has to consider that in the fluid a minor contribution of electron transfer (≤5%) can be masked by experimental uncertainties; moreover, the pattern of photoinduced processes can be slightly different in the two environments. Indeed, the efficiencies of the photovoltaic devices are low, namely from 0.01 to 0.03%. We believe that this is a consequence of the prevalence of energy transfer vs electron transfer, thus the main part of the light energy absorbed by the OPV fragment is promptly conveyed to the fullerene lowest singlet excited state, in analogy with the behavior in fluid solution. In turn, the fullerene lowest singlet and triplet excited states cannot yield charge separation, due to their low energy content (Figure 4); thus electron/hole pairs cannot be generated anymore. Therefore, only a small part of the absorbed light is able to contribute effectively to the photocurrent. Nevertheless, the molecular approach to photovoltaic cells for solar energy conversion appears to be promising, since the bicontinuous network obtained by chemically linking the hole-conducting OPV moiety to the electron-conducting fullerene subunit prevents any problems arising from bad contacts at the junction, as observed for OPV/C_{60} blends. Furthermore, the behavior of a unique molecule in a photovoltaic cell and the study of its electronic properties allows to obtain easily structure/activity relationships for a better understanding for the photovoltaic system. The light-collecting and energy-conversion efficiencies of the molecular photovoltaic system are not yet optimized, and further improvements could be expected by the utilization of new fullerene derivatives with a strong absorption in the visible range and able to achieve efficient and very fast photoinduced charge separation. Work in this direction is underway in our laboratories.

Experimental Section

General Methods. Reagents and solvents were purchased as reagent grade and used without further purification. All reactions were performed in standard glassware under an inert Ar atmosphere. Evaporation and concentration were done at water aspirator pressure and drying in vacuo at 10^{-2} Torr. Column chromatography: silica gel 60 (230−400 mesh, 0.040−0.063 mm) was purchased from E. Merck. Thin layer chromatography (TLC) was performed on glass sheets coated with silica gel 60 F_{254} purchased from E. Merck, visualization by UV light. Melting points were measured on an electrothermal digital melting point apparatus and are uncorrected. UV/vis spectra (λ_{max} in nm (ϵ)) were measured on a Hitachi U-3000 spectrophotometer. IR spectra (cm^{-1}) were measured on an ATI Mattson Genesis Series FTIR instrument. NMR spectra were recorded on a Bruker AC 200 (200 MHz) or a Bruker AM 400 (400 MHz) with solvent peaks as reference. FAB-mass spectra (*m*/*z*; % relative intensity) were taken on a ZA HF instrument with 4-nitrobenzyl alcohol as matrix. Elemental analyses were performed by the analytical service at the Institut Charles Sadron (Strasbourg, France).

3,5-Didodecyloxybenzyl Alcohol (1). A mixture of 3,5-dihydroxybenzyl alcohol (15.0 g, 108 mmol), K_2CO_3 (62.7 g, 453 mmol), and 1-bromododecane (56.84 g, 228 mmol) in DMF (220 mL) was heated at 70 °C for 48 h. After cooling, the resulting mixture was filtered and evaporated to dryness. The brown residue was taken up in CH_2Cl_2. The organic layer was washed with a saturated aqueous NaCl solution and then with water, dried ($MgSO_4$), filtered, and evaporated to dryness. Recrystallization from hexane yielded **1** (36.2 g, 70%) as colorless crystals (mp 39 °C). IR (CH_2Cl_2): 3607 (O−H). ^{1}H NMR (200 MHz, $CDCl_3$): 6.51 (d, J = 2 Hz, 2 H), 6.39 (t, J = 2 Hz, 1 H), 4.60 (s, 2 H), 3.93 (t, J = 6.5 Hz, 4 H), 1.80−1.70 (m, 4 H), 1.50−1.20 (m, 36 H), 0.90 (t, J = 6.5 Hz, 6 H). ^{13}C NMR (50 MHz, $CDCl_3$): 160.50, 143.18, 105.02, 100.52, 68.03, 65.44, 31.90, 29.58, 29.36, 29.24, 26.02, 22.67, 14.09. Anal. Calcd for $C_{31}H_{56}O_3$ (476.8): C 78.09, H 11.84. Found: C 78.09, H 12.04.

3,5-Didodecyloxybenzaldehyde (2). A mixture of **1** (6.5 g, 13.6 mmol) and MnO_2 (30 g) in CH_2Cl_2 (250 mL) was stirred at room temperature for 1 h. After addition of $MgSO_4$ (30 g), the mixture was filtered and the filtrate evaporated to dryness. Column chromatography (SiO_2, CH_2Cl_2/hexane 1:1) gave **2** (5.70 g, 90%) as colorless crystals (mp 39 °C). ^{1}H NMR (200 MHz, $CDCl_3$): 9.71 (s, 1 H), 6.99 (d, J = 2 Hz, 2 H), 6.70 (t, J = 2 Hz, 1 H), 3.99 (t, J = 6.5 Hz, 4 H), 1.80 (m, 4 H), 1.50−1.20 (m, 36 H), 0.90 (t, J = 6.5 Hz, 6 H). ^{13}C NMR (50 MHz, $CDCl_3$): 192.02, 160.71, 138.28, 107.95, 107.52, 68.38, 31.90, 29.63, 29.57, 29.34, 29.12, 25.99, 22.67, 14.09.

(*E*)-*N*-Phenyl-3,5-didodecyloxybenzaldimine (3). A solution of **2** (6.3 g, 13.4 mmol) and aniline (1.34 mL, 14.7 mmol) in benzene (100 mL) was refluxed for 24 h using a Dean−Stark trap. After cooling, the solution was evaporated to dryness and recrystallization from EtOH yielded **3** (6.61 g, 90%) as colorless crystals (mp 39 °C). ^{1}H NMR (200 MHz, $CDCl_3$): 8.35 (s, 1 H), 7.44−7.18 (m, 5 H), 7.04 (d, J = 2 Hz, 2 H), 6.58 (t, J = 2 Hz, 1 H), 3.99 (t, J = 6.5 Hz, 4 H), 1.80 (m, 4 H), 1.50−1.20 (m, 36 H), 0.90 (t, J = 6.5 Hz, 6 H). ^{13}C NMR (50 MHz, $CDCl_3$): 160.52, 160.43, 151.97, 138.02, 129.08, 125.86, 120.82, 106.84, 104.95, 68.21, 31.90, 29.61, 29.36, 29.21, 26.02, 22.67, 14.10.

1-Bromo-4-(4,4-dimethyl-2,6-dioxan-1-yl)benzene (4). A solution of *p*-bromobenzaldehyde (15 g, 81 mmol), 2,2-dimethylpropane-1,3-diol (16.88 g, 162 mmol), and *p*-TsOH (50 mg) in benzene (100 mL) was refluxed for 24 h using a Dean−Stark trap. After cooling, the solution was evaporated to dryness and column chromatography (SiO_2, hexane/CH_2Cl_2 7:3) gave **4** (20.8 g, 95%) as colorless crystals (mp 62 °C). ^{1}H NMR (200 MHz, $CDCl_3$): 7.52 (d, J = 9 Hz, 2H), 7.45 (d, J = 9 Hz, 2H), 5.35 (s, 1 H), 3.70 (AB, J = 10.5 Hz, 4 H), 1.28 (s, 3 H), 0.81 (s, 3 H). ^{13}C NMR (50 MHz, $CDCl_3$): 137.48, 131.32, 127.87, 127.23, 122.77, 100.83, 77.54, 30.14, 22.96, 21.78.

4-(4,4-Dimethyl-2,6-dioxan-1-yl)benzaldehyde (5). A 1.5 M solution of *t*-BuLi in hexane (72 mL, 108 mmol) was slowly added to a

degassed solution of **4** (13.3 g, 49 mmol) in dry THF (130 mL) at −78 °C under Ar. After 30 min at −78 °C, the solution was allowed to warm to 0 °C (over 1 h) and cooled again to −78 °C. Dry DMF (7.6 mL, 98 mmol) was then added and the resulting mixture allowed to warm to 0 °C (over 1 h). An aqueous 1 M HCl solution (60 mL) was added and the mixture was concentrated. The aqueous layer was extracted twice with CH_2Cl_2. The combined organic layers were washed with water, dried ($MgSO_4$), and evaporated to dryness. Column chromatography (SiO_2, hexane/CH_2Cl_2 7:3) gave **5** (10.5 g, 98%) as colorless crystals (mp 65 °C). ^{1}H NMR (200 MHz, $CDCl_3$): 9.59 (s, 1H), 7.90 (d, J = 9 Hz, 2 H), 7.67 (d, J = 9 Hz, 2 H), 5.45 (s, 1 H), 3.74 (AB, J = 10.5 Hz, 4 H), 1.29 (s, 3 H), 0.82 (s, 3 H). ^{13}C NMR (50 MHz, $CDCl_3$): δ 192.06, 144.54, 136.62, 129.74, 126.91, 100.71, 77.66, 53.41, 30.27, 22.99, 21.84.

(*Z*)-1-[4-(4,4-Dimethyl-2,6-dioxan-1-yl)phenyl]-2-(4-methylphenyl)ethene (*Z*-6) and (*E*)-1-[4-(4,4-Dimethyl-2,6-dioxan-1-yl)phenyl]-2-(4-methylphenyl)ethene (*E*-6). A mixture of **5** (5.0 g, 22.6 mmol), (4-methylbenzyl)triphenylphosphonium chloride (9.14 g, 22.6 mmol), and *t*-BuOK (2.94 g, 24.9 mmol) in EtOH (30 mL) was stirred at room temperature for 1 h under Ar. A saturated aqueous NH_4Cl solution was then added and the mixture concentrated. The aqueous layer was extracted twice with CH_2Cl_2. The combined organic layers were washed with water and dried ($MgSO_4$) and evaporated to dryness. Column chromatography (SiO_2, hexane/CH_2Cl_2 6:4) gave **6** as an *E*:*Z* isomer mixture in a 55:45 ratio. Both isomers could be isolated in a pure form by column chromatography on SiO_2 and characterized. In a preparative procedure, the *E*:*Z* mixture obtained after the first chromatographic purification was directly isomerized as follows: a solution of the *E*:*Z* mixture and I_2 (100 mg) in toluene was refluxed for 12 h and then cooled to room temperature. The resulting toluene solution was washed with an aqueous 0.3 M $Na_2S_2O_6$ solution and water, dried ($MgSO_4$), filtered, and evaporated to dryness. Column chromatography (SiO_2, hexane/CH_2Cl_2 6:4) gave *E*-**6** (4.9 g, 70% from **5**).

***Z*-6**. ^{1}H NMR (200 MHz, $CDCl_3$): 7.37 (d, J = 9 Hz, 2 H), 7.28 (d, J = 9 Hz, 2 H), 7.15 (d, J = 9 Hz, 2 H), 6.01 (d, J = 9 Hz, 2 H), 6.54 (AB, J = 12 Hz, 2 H), 5.36 (s, 1 H), 3.70 (AB, J = 10.5 Hz, 4 H), 2.31 (s, 3 H), 1.30 (s, 3 H), 0.80 (s, 3 H). ^{13}C NMR (50 MHz, $CDCl_3$): 138.02, 137.00, 136.81, 134.02, 130.39, 129.08, 128.86, 128.73, 125.99, 101.64, 77.60, 30.14, 22.99, 21.81, 21.17. Anal. Calcd for $C_{21}H_{24}O_2$ (308.4): C 81.78, H 7.84; Found: C 81.86, H 7.79.

***E*-6.** ^{1}H NMR (200 MHz, $CDCl_3$): 7.50 (s, 4 H), 7.42 (d, J = 8 Hz, 2 H), 7.17 (d, J = 8 Hz, 2 H), 7.08 (s, 2 H), 5.40 (s, 1 H), 3.70 (AB, J = 10.5 Hz, 4 H), 2.36 (s, 3 H), 1.31 (s, 3 H), 0.81 (s, 3 H). ^{13}C NMR (50 MHz, $CDCl_3$): 138.04, 137.51, 134.42, 130.20, 129.53, 129.37, 128.89, 127.30, 126.82, 126.41, 126.27, 101.54, 77.63, 30.22, 23.03, 21.87, 21.24. Anal. Calcd for $C_{21}H_{24}O_2$ (308.4): C 81.78, H 7.84. Found: C 81.84, H 7.79.

(*E*)-1-(4-Formylphenyl)-2-(4-methylphenyl)ethene (*E*-7). A mixture of *p*-bromobenzaldehyde (8.0 g, 43.2 mmol), *p*-methylstyrene (5.62 g, 47.5 mmol), $Pd(OAc)_2$ (291 mg, 1.3 mmol), and POT (789 mg, 2.6 mmol) in Et_3N/xylene 1:1 (100 mL) was heated to 130 °C under Ar for 48 h. After cooling, the resulting mixture was filtered and evaporated. The brown residue was taken up in CH_2Cl_2. The organic layer was washed with water, dried ($MgSO_4$), filtered, and evaporated to dryness. Column chromatography (SiO_2, hexane/CH_2Cl_2 6:4) gave *E*-**7** (6.76 g, 70%). ^{1}H NMR (200 MHz, $CDCl_3$): 9.61 (s, 1H), 7.87 (AB, J = 8.5 Hz, 2 H), 7.65 (AB, J = 8.5 Hz, 2 H), 7.46 (AB, J = 8.5 Hz, 2 H), 7.22 (AB, J = 8.5 Hz, 2 H), 7.18 (AB, J = 16 Hz, 2 H), 2.38 (s, 3 H). ^{13}C NMR (50 MHz, $CDCl_3$): 191.58, 143.60, 138.56, 135.08, 133.71, 132.12, 130.20, 129.53, 126.81, 126.72, 126.25, 21.30. Anal. Calcd for $C_{16}H_{14}O$ (222.3): C 86.45, H 6.35. Found: C 86.43, H 6.36.

***(E)*-1-[4-(4,4-Dimethyl-2,6-dioxan-1-yl)phenyl]-2-(4-methylphenyl)ethene (*E*-6) from *E*-7.** A solution of *E*-**7** (2.5 g, 11.3 mmol), 2,2-dimethylpropane-1,3-diol (2.36 g, 22.7 mmol), and *p*-TsOH (50 mg) in benzene (100 mL) was refluxed for 24 h using a Dean−Stark trap. After cooling, the solution was evaporated to dryness and column chromatography (SiO_2, hexane/CH_2Cl_2 7:3) gave *E*-**6** (3.31 g, 95%) as colorless crystals (mp 166 °C).

Compound 3PV. *t*-BuOK (8.94 g, 75 mmol) was added to a solution of **3** (11.46 g, 20.9 mmol) and *E*-**6** (6.45 g, 20.9 mmol) in dry DMF (30 mL) under argon at 80 °C. The mixture was stirred for 1 h at 80 °C and, after cooling, it was poured into an aqueous 0.5 M HCl solution (500 mL). The mixture was extracted with CH_2Cl_2. The organic layer was washed with water, dried ($MgSO_4$), and evaporated to dryness. Column chromatography (SiO_2, CH_2Cl_2/hexane 1:1) gave **3PV** (14.55 g, 91%) as yellow crystals (mp 82 °C). ^{1}H NMR (200 MHz, $CDCl_3$): 7.51 (m, 8 H), 7.12 (s, 2 H), 7.06 (s, 2 H), 6.66 (d, J = 2 Hz, 2 H), 6.39 (t, J = 2 Hz, 1 H), 5.41 (s, 1 H), 3.98 (t, J = 6.5 Hz, 4 H), 3.70 (AB, J = 10.5 Hz, 4 H), 1.79−1.76 (m, 4 H), 1.43−1.27 (m, 39 H), 0.90 (t, J = 6.5 Hz, 6 H), 0.82 (s, 3 H). ^{13}C NMR (50 MHz, $CDCl_3$): 160.43, 139.08, 137.75, 136.54, 129.31, 128.64, 128.48, 128.13, 127.23, 126.79, 126.43, 126.21, 105.01, 101.44, 100.88, 77.57, 67.96, 31.88, 30.14, 29.58, 29.37, 29.31, 29.26, 26.02, 22.99, 22.64, 21.81, 14.09. UV−vis (CH_2Cl_2): see Table 2. Anal. Calcd for $C_{52}H_{76}O_4$ (765.2): C 81.62, H 10.01. Found: C 81.51, H 10.01.

Compound 8. A mixture of **3PV** (8.0 g, 10.4 mmol) and CF_3CO_2H (80 mL) in CH_2Cl_2/H_2O 1:1 (150 mL) was stirred at room temperature for 5 h. The organic layer was then washed with water (4×), dried ($MgSO_4$), and evaporated to dryness. Column chromatography (SiO_2, CH_2Cl_2/hexane 1:1) gave **8** (6.98 g, 96%). ^{1}H NMR (200 MHz, $CDCl_3$): 9.60 (s, 1 H), 7.88 (d, J = 9.5 Hz, 2 H), 7.67 (d, J = 9.5 Hz, 2 H), 7.55 (m, 4 H), 7.22 (q, J = 16.5 Hz, 2 H), 7.08 (s, 2 H), 6.66 (d, J = 2 Hz, 2 H), 6.39 (t, J = 2 Hz, 1 H) 3.98 (t, J = 6.5 Hz, 4 H), 1.79−1.76 (m, 4 H), 1.43−1.27 (m, 36 H), 0.90 (t, J = 6.5 Hz, 6 H). ^{13}C NMR (50 MHz, $CDCl_3$): 191.59, 160.48, 143.38, 138.95, 137.45, 135.80, 135.24, 131.70, 130.20, 129.28, 128.26, 127.23, 127.05, 126.94, 126.83, 105.12, 101.01, 68.06, 31.90, 29.62, 29.35, 29.28, 26.06, 22.67, 14.12. UV−vis (CH_2Cl_2): 232 (24708), 375 (58143). Anal. Calcd for $C_{47}H_{66}O_3$ (679.0): C 83.13, H 9.80. Found: C 83.08, H 9.83.

Compound 9. A mixture of **8** (800 mg, 1.17 mmol), *t*-BuOK (153 mg, 1.29 mmol), and methyltriphenylphosphonium bromide (472 mg, 1.29 mmol) in dry THF (5 mL) was stirred at room temperature for 1 h. A saturated aqueous NH_4Cl solution was then added and the resulting mixture was concentrated. The aqueous layer was extracted twice with CH_2Cl_2. The combined organic layers were washed with water, dried ($MgSO_4$), and evaporated to dryness. Column chromatography (SiO_2, CH_2Cl_2/hexane 1:3) gave **9** (650 mg, 82%). ^{1}H NMR (200 MHz, $CDCl_3$): 7.50−7.39 (m, 8 H), 7.12 (s, 2 H), 7.06 (s, 2 H), 6.75 (m, 1 H), 6.66 (d, J = 2 Hz, 2 H), 6.39 (t, J = 2 Hz, 1 H), 5.78 (d, J = 17.5 Hz, 1 H), 5.26 (d, J = 11.5 Hz, 1 H), 3.98 (t, J = 6.5 Hz, 4 H), 1.79−1.76 (m, 4 H), 1.43−1.27 (m, 36 H), 0.90 (t, J = 6.5 Hz, 6 H). ^{13}C NMR (50 MHz, $CDCl_3$): 160.46, 139.11, 136.85, 136.65, 136.57, 136.40, 128.70, 128.48, 128.12, 126.84, 126.65, 126.53, 113.70, 105.05, 100.90, 68.03, 31.91, 30.27, 29.61, 29.40, 29.34, 29.28, 26.06, 22.68, 14.12.

Compound 10. A mixture of **9** (650 mg, 0.96 mmol), 4-bromobenzaldehyde (177 mg, 0.96 mmol), $Pd(OAc_2)$ (9 mg, 0.04 mmol), and POT (58 mg, 0.19 mmol) in Et_3N/xylene 1:1 (8 mL) was stirred under Ar at 130 °C for 48 h. After cooling, the resulting mixture was filtered and evaporated. The brown residue was taken up in CH_2Cl_2. The organic layer was washed with water, dried ($MgSO_4$), filtered, and evaporated to dryness. Column chromatography (SiO_2, hexane/CH_2Cl_2 6:4) gave **10** (450 mg, 60%) as yellow crystals (mp 160 °C). ^{1}H NMR (200 MHz, $CDCl_3$): 9.59 (s,1 H), 7.89 (d, J = 8.5 Hz, 2 H), 7.67 (d, J = 8.5 Hz, 2 H), 7.55 (m, 8 H), 7.22 (q, J = 16.5 Hz, 2 H), 7.15 (s, 2 H), 7.07 (s, 2 H), 6.66 (d, J = 2 Hz, 2 H), 6.39 (t, J = 2 Hz, 1 H) 3.98 (t, J = 6.5 Hz, 4 H), 1.79−1.76 (m, 4 H), 1.43−1.27 (m, 36 H), 0.90 (t, J = 6.5 Hz, 6 H). ^{13}C NMR (50 MHz, $CDCl_3$): 191.60, 160.46, 143.39, 139.08, 137.55, 136.75, 136.49, 135.79, 135.21, 131.70, 130.59, 130.24, 128.82, 128.69, 128.43, 127.85, 127.27, 127.05, 126.89, 118.59, 105.07, 100.92, 68.05, 34.26, 31.90, 29.61, 29.35, 29.28, 26.05, 22.67, 19.65, 14.12. IR (CH_2Cl_2): 1641 (C═O). UV−vis (CH_2Cl_2.): 227 (27295), 284 (12927), 396 (82866). Anal. Calcd for $C_{55}H_{72}O_3$ (781.2): C 84.57, H 9.29. Found: C 84.22 H 9.43.

Compound 4PV. A solution of **8** (800 mg, 1.17 mmol), *t*-BuOK (153 mg, 1.32 mmol), and (4-methylbenzyl)triphenylphosphonium chloride (472 mg, 1.32 mmol) in dry THF (20 mL) was stirred under Ar at room temperature for 2 h. A saturated aqueous NH_4Cl solution was then added and the mixture concentrated. The aqueous layer was extracted twice with CH_2Cl_2. The combined organic layers were washed with water, dried ($MgSO_4$), and evaporated to dryness to give a mixture

of two isomers. Isomerization was achieved as follows: a solution of the crude mixture and I_2 (50 mg) in toluene (50 mL) was refluxed for 12 h and then cooled to room temperature. The resulting toluene solution was washed with an aqueous 0.3 M $Na_2S_2O_6$ solution and water, dried ($MgSO_4$), filtered, and evaporated to dryness. Column chromatography (SiO_2, hexane/CH_2Cl_2 4:1) gave **4PV** (378 mg, 42%) as yellow crystals (mp 173 °C). ^{1}H NMR (200 MHz, $CDCl_3$): 7.54−7.39 (m, 10 H), 7.20−7.05 (m, 8 H), 6.70 (d, J = 2 Hz, 2 H), 6.42 (t, J = 2 Hz, 1 H) 3.98 (t, J = 6.5 Hz, 4 H), 2.38 (s, 3 H), 1.79−1.76 (m, 4 H), 1.43−1.27 (m, 36 H), 0.90 (t, J = 6.5 Hz, 6 H). ^{13}C NMR (50 MHz, $CDCl_3$): 160.48, 139.14, 138.09, 137.54, 136.87, 136.72, 136.52, 136.43, 136.26, 134.65, 134.49, 130.21, 129.40, 129.11, 128.67, 128.51, 128.16, 127.96, 127.57, 127.21, 126.80, 126.72, 126.41, 126.28, 105.04, 100.89, 68.04, 53.41, 31.91, 29.61, 29.40, 29.35, 29.28, 26.06, 22.68, 21.26, 14.12. UV−vis (CH_2Cl_2): see Table 2. Anal. Calcd for $C_{55}H_{74}O_2$ (767.2): C 86.11, H 9.72. Found: C 85.76 H 9.78.

Fulleropyrrolidine C_{60}−3PV. A mixture of **8** (400 mg, 0.58 mmol), C_{60} (467 mg, 0.64 mmol), and sarcosine (420 mg, 4.70 mmol) in toluene (500 mL) was refluxed under Ar for 16 h. After cooling, the resulting solution was evaporated to dryness and column chromatography (SiO_2, hexane/toluene 1:1) gave **C_{60}−3PV** (366 mg, 43%) as a brown solid (mp 104 °C). ^{1}H NMR (400 MHz, $CDCl_3$): 7.82 (br, 2 H), 7.61 (d, J = 8 Hz, 2 H), 7.48 (s, 4 H), 7.12 (AB, J = 17 Hz, 2 H), 7.04 (AB, J = 17 Hz, 2 H), 6.65 (d, J = 1.5 Hz, 2 H), 6.38 (t, J = 1.5 Hz, 1 H) 5.00 (d, J = 9.5 Hz, 1 H), 4.94 (s, 1 H), 4.25 (d, J = 9.5 Hz, 1 H), 3.96 (t, J = 5 Hz, 4 H), 2.83 (s, 3 H), 1.78 (m, 4 H), 1.26−1.31 (m, 36 H), 0.90 (t, J = 5.5 Hz, 6 H). ^{13}C NMR (100 MHz, $CDCl_3$): 160.50, 156.20, 153.98, 153.37, 147.28, 146.71, 146.46, 146.30, 146.27, 146.17, 146.10, 146.05, 145.92, 145.74, 145.52, 145.28, 145.14, 144.69, 144.58, 144.37, 143.13, 142.98, 142.66, 142.54, 142.27, 142.23, 142.15, 142.10, 142.05, 142.02, 141.95, 141.91, 141.84, 141.67, 141.52, 140.14, 139.89, 139.56, 139.15, 137.44, 136.82, 136.71, 136.60, 136.55, 136.43, 135.89, 135.77, 129.68, 128.86, 128.71, 128.54, 128.12, 126.90, 105.17, 101.03, 83.35, 70.00, 69.06, 68.10, 40.05, 31.93, 29.69, 29.66, 29.63, 29.44, 29.34, 26.11, 22.71, 14.15. UV−vis (CH_2Cl_2): see Table 2. FAB-MS: 1426.8 (13, $[M + H]^+$, calcd for $C_{109}H_{72}O_2N$ 1426.6), 720.2 (96, $[C_{60}]^+$, calcd for C_{60} 720.0), 705.6 (100, $[M - C_{60}]^+$, calcd for $C_{49}H_{71}O_2N$ 705.5). Anal. Calcd for $C_{109}H_{71}O_2N$ (1426.8): C 91.76, H 5.02, N 0.98. Found: C 91.27 H 5.09, N 1.07.

Fulleropyrrolidine C_{60}−4PV. A mixture of **10** (180 mg, 0.23 mmol), C_{60} (182 mg, 0.25 mmol), and sarcosine (182 mg, 2.02 mmol) in toluene (200 mL) was refluxed under Ar for 16 h. After cooling, the resulting solution was evaporated to dryness and column chromatography (SiO_2, hexane/toluene 1:1) gave **C_{60}−4PV** (139 mg, 40%) as a brown solid (mp >200 °C). ^{1}H NMR (400 MHz, $CDCl_3$): 7.82 (br, 2 H), 7.61 (d, J = 8 Hz, 2 H), 7.48 (s, 8H), 7.12 (AB, J = 17 Hz, 2 H), 7.13 (s, 2 H), 7.08 (AB, J = 17 Hz, 2 H), 6.68 (d, J = 1.5 Hz, 2 H), 6.41 (t, J = 1.5 Hz, 1 H) 5.00 (d, J = 9.5 Hz, 1 H), 4.96 (s, 1 H), 4.28 (d, J = 9.5 Hz, 1 H), 3.99 (t, J = 5 Hz, 4 H), 2.84 (s, 3 H), 1.81 (m, 4 H), 1.50−1.29 (m, 36 H), 0.91 (t, J = 5.5 Hz, 6 H). ^{13}C NMR (100 MHz, $CDCl_3$): 160.57, 154.08, 153.48, 153.41, 147.35, 146.80, 146.52, 146.32, 146.25, 145.99, 145.82, 145.59, 145.38, 145.32, 145.21, 144.45, 143.19, 142.73, 142.62, 142.30, 142.18, 141.98, 141.91, 140.20, 139.21, 137.53, 136.87, 136.76, 136.72, 136.65, 136.59, 136.50, 135.79, 129.75, 128.84, 128.75, 128.59, 128.30, 128.18, 126.94, 126.90, 105.20, 101.07, 83.47, 70.10, 69.14, 68.15, 40.08, 31.96, 29.71, 29.68, 29.65, 29.45, 29.39, 26.13, 22.73, 14.15. UV−vis (CH_2Cl_2): see Table 2. FAB-MS: 1528.6 (17, $[M + H]^+$, calcd for $C_{117}H_{77}O_2N$ 1528.6), 807.6 (100, $[M - C_{60}]^+$, calcd for $C_{57}H_{77}O_2N$ 807.6), 720.0 (92, $[C_{60}]^+$, calcd for C_{60} 720.0). Anal. Calcd for $C_{117}H_{77}O_2N$ (1528.9): C 91.91, H 5.08, N 0.92. Found: C 91.68 H 5.15, N 0.92.

Fulleropyrrolidine FP. A mixture of **2** (238 mg, 0.50 mmol), C_{60} (400 mg, 0.55 mmol), and sarcosine (444 mg, 5.00 mmol) in toluene (400 mL) was refluxed under Ar for 16 h. After cooling, the resulting solution was evaporated to dryness and column chromatography (SiO_2, hexane/toluene 1:1) gave **FP** (254 mg, 42%) as a brown solid (mp 105 °C). ^{1}H NMR (400 MHz, $CDCl_3$): 7.04 (d, J = 1.5 Hz, 2 H), 6.48 (t, J = 1.5 Hz, 1 H) 5.02 (d, J = 9.5 Hz, 1 H), 4.90 (s, 1 H), 4.31 (d, J = 9.5 Hz, 1 H), 4.02 (t, J = 5 Hz, 4 H), 2.90 (s, 3 H), 1.81 (m, 4 H), 1.50−1.29 (m, 36 H), 0.91 (t, J = 5.5 Hz, 6 H). ^{13}C NMR (50 MHz, $CDCl_3$): 160.29, 156.08, 154.04, 153.69, 153.42, 147.25, 147.02, 146.42, 146.24, 146.16, 146.07, 145.90, 145.74, 145.48, 145.21, 145.11, 144.65, 144.60, 144.34, 143.10, 142.93, 142.62, 142.52, 142.17, 141.98, 141.88, 141.76, 141.63, 141.55, 140.13, 140.07, 139.74, 139.56, 138.99, 136.58, 136.37, 135.75, 101.89, 83.68, 69.91, 68.99, 68.17, 40.10, 31.90, 29.64, 29.41, 29.35, 29.14, 26.02, 22.69, 14.15. UV−vis (CH_2Cl_2): see Table 2. Anal. Calcd for $C_{93}H_{59}O_2N$ (1222.5): C 91.37, H 4.86, N 1.15. Found: C 91.41 H 4.88, N 1.14.

Electrochemical Measurements. CV and OSWV were performed on a Windows-driven BAS 100W electrochemical analyzer (Bioanalytical Systems, West Lafayette, IN) at room temperature with a three-electrode configuration in *o*-dichlorobenzene (*o*-ODCB) solution containing the substrate (0.3−0.8 mmol dm^{-3}) and *n*-Bu_4NPF_6 as supporting electrolyte. A glassy carbon (GC, ∅ 3 mm) disk served as the working electrode, with a platinum wire (∅ 1 mm) and a commercial Ag/AgCl aqueous electrode as the counter and the reference electrode, respectively. Both the counter and the reference electrodes were directly immersed in the electrolyte solution. The surface of the working electrode was polished before each measurement with commercial Alpha Micropolish Alumina No. 1C (Aldrich) with a particle size of 1.0 μm. Tetrabutylammonium hexafluorophosphate (*n*-Bu_4NPF_6) purchased from Fluka (>99%) was recrystallized twice from ethanol and dried in a vacuum overnight prior to use and was employed as the supporting electrolyte in 0.1 mol dm^{-3} concentration. Solutions were stirred and deaerated by bubbling argon for a few minutes prior to each voltammetric measurement. The scan rate was 100 mV s^{-1} unless otherwise specified. OSWVs were obtained using a sweep width of 25 mV, a frequency of 15 Hz, a step potential of 4 mV, a S. W. amplitude of 25 mV, and a quiet time of 2 s.

Spectroscopic and Photophysical Measurements. The solvent used for the photophysical investigations is spectrofluorimetric grade CH_2Cl_2 and benzonitrile (Carlo Erba). Absorption spectra were recorded with a Perkin-Elmer Lambda 5 spectrophotometer. Uncorrected emission spectra were obtained with a Spex Fluorolog II spectrofluorimeter eqipped with a continuous 150 W Xe lamp as excitation source and a Hamamatsu R-928 photomultiplier tube as detector. The corrected spectra were obtained via a calibration curve determined by means of a 45 W quartz-halogen tungsten filament lamp (Optronic Laboratories) calibrated in the range 400−1800 nm. Fluorescence quantum yields were measured with the method described by Demas and Crosby[37] using as standards quinine sulfate in 1 N H_2SO_4 (Φ = 0.546)[38] and $[Os(phen)_3]^{2+}$ in acetonitrile (Φ_{em} = 0.005).[39] To record the 77 K luminescence spectra the samples were put in glass tubes (2 mm diameter) and inserted in a special quartz dewar, filled up with liquid nitrogen. When needed, spectra of pure dichloromethane solvent were recorded and then subtracted as background signal, to eliminate the contribution of the light scattered by the rigid matrix. Phosphorescence and corrected excitation spectra (the latter can be obtained only for $\lambda \geq 300$ nm) were recorded with a Perkin-Elmer LS-50B spectrofluorimeter (pulsed Xe lamp).

Emission lifetimes were determined with an IBH single photon counting spectrometer equipped with a thyratron gated nitrogen lamp working at 40 kHz (λ_{exc} = 337 nm, 0.5 ns time resolution after deconvolution of the flash profile); the detector was a red-sensitive (185−850 nm) Hamamatsu R-3237-01 photomultiplier tube.

Experimental uncertainties are estimated to be ±7% for lifetime determination, ±15% for quantum yields, and ±3 nm for emission and absorption peaks.

Device Preparation. Compounds **C_{60}−3PV** and **C_{60}−4PV** were spin-coated (1000−2000 rpm) from 4% weight $CHCl_3$ solutions on ITO/glass substrates at room temperature. Typical thicknesses were between 100 and 140 nm. The Al electrode was vacuum evaporated on the films to a thickness of 100 nm.

Photovoltaic Characterization. The second harmonic of a Ti:sapphire laser (Coherent, Mira 900) together with I−V source-measure unit (Keithley, model 236) were employed. All measurements were done under dynamic vacuum better than 10^{-6} Torr.

(37) Demas, J. N.; Crosby, G. A. *J. Phys. Chem.* **1971**, *93*, 2841.
(38) Meech, S. R.; Philips, D. J. *J. Photochem.* **1983**, *23*, 193.
(39) Kober, E. M.; Caspar, J. V.; Lumpkin, R. S.; Meyer, T. J. *J. Phys. Chem.* **1986**, *90*, 3722.

Morphology Characterization. Compounds **C_{60}−3PV** and **C_{60}−4PV** were spin-coated from 4% weight $CHCl_3$ solutions on cleaved mica and examined by AFM by using a Digital Nanoscope III. Silicon cantilevers were used to acquire topography images in Tapping Mode at room temperature under ambient conditions.

Acknowledgment. This paper is dedicated to Prof. Fred Wudl on the occasion of his 60th birthday. This research was supported by the French CNRS and ECODEV, the Italian CNR, and CW/STW. We also wish to thank the U.S. National Science Foundation, Grant CHE-9816503, for generous financial support to S.-G.L. and L.E. We thank Hoechst AG for samples of C_{60}, Dr. A. Van Dorsselaer, R. Hueber. and H. Nierengarten for recording the mass spectra, J.-D. Sauer for high-field NMR, and L. Oswald for technical help.

JA9941072